Monte Carlo Studies of Isomers, Structures, and Properties in Benzene−Cyclohexane Clusters: Computation Strategy and Application to the Dimer and Trimer, $(C_6H_6)(C_6H_{12})_n$, $n = 1-2$

David C. Easter,* David A. Terrell, and Jessica A. Roof

Department of Chemistry and Biochemistry, Texas State University, San Marcos, Texas 78666

Received: October 21, 2004; In Final Form: November 5, 2004

Low-temperature isomeric energies, structures, and properties of benzene−cyclohexane clusters are investigated via Monte Carlo simulations. The Monte Carlo strategy is first documented and then applied to (C_6H_6)-(C_6H_{12}) and $(C_6H_6)(C_6H_{12})_2$ using four different potential energy surfaces. Results identify a single parallel-displaced dimer isomer. MP2 optimizations and frequency calculations support the Monte Carlo dimer structure and identify the van der Waals mode observed in vibronic spectra. Caloric simulations identify two temperatures where structural transitions occur and imply an experimental temperature below 10 K for dimers in cold supersonic expansions. The $(C_6H_6)(C_6H_{12})_2$ studies identify eight independent trimer isomers: three form parallel-stacked (sandwich) arrangements with the two cyclohexane moieties related through a D_{6h} transformation. The remaining five trimer isomers are trigonal, with no overall symmetry. Caloric studies indicate that the sandwich and trigonal isomeric classes coexist independently below 60 K, consistent with trimer vibronic spectra that contain two independent van der Waals progressions.

I. Introduction

Clusters are of fundamental importance because of their unique physical and chemical properties and their role as bridges in the evolution of properties from the molecular to the bulk. Molecular clusters bound together through weak van der Waals (vdW) interactions can be profitably examined to obtain information regarding physical structures and intermolecular motions. Van der Waals systems are characterized by small interactions amenable to modeling by pairwise additive atom−atom potentials. Furthermore, in benzene clusters, vdW cluster modes have been observed to be separable from and uncoupled to the molecular ring modes of the cluster members.[1] VdW modes are generally low in frequency and play an important part in intramolecular vibration redistribution and other dynamical processes.[2]

As the aromatic prototype, neat benzene clusters have received attention both experimentally[1,3−12] and theoretically[13−19] largely because several twelve-site atom−atom potential energy parameter sets applicable to benzene clusters have been developed that enable the correlation of experimental data with theoretical predictions.[13,16,18,20−23] Isotopic substitution experiments applied to benzene clusters have provided information about solvent−solute interactions[4,5] and the dynamics of free jet cluster formation.[3] While progress has been realized through neat benzene cluster studies, an extension to solvent−solute cluster systems containing benzene promises significant new information.

Benzene−cyclohexane clusters containing a single C_6H_6 moiety represent such a system. Experimental and computational results from $(C_6H_6)(C_6H_{12})_n$ can be directly compared to existing $(C_6H_6)(C_6D_6)_n$ data to assess how the solvent's monomer structure and other properties (e.g., aromaticity) affect overall cluster properties. Mass dependence is eliminated as a variable in the analysis because both solvents, (C_6H_{12}) and (C_6D_6), have the same molecular mass. Furthermore, when probed in the appropriate region near 260 nm, the C_6H_6 $B_{2u} \leftarrow A_{1g}$ vibronic transitions (0^0_0 and 6^1_0) are well-separated from those of the C_6H_{12} solvent, providing a probe of the environment and properties of the C_6H_6 chromophore.

More than a decade ago, El-Shall and Whetten reported resonant two-photon ionization (R2PI) spectra of benzene−cyclohexane clusters measured through the 6^0_1 vibronic transition of benzene.[24] They found support for a structural shell-filling model and assigned two sharp features in the (C_6H_6)-$(C_6H_{12})_6$ spectrum to unique sites in a pentagonal bipyramid structure. Sharp features in their spectra rested on a broad amorphous base, implying the existence of "warm" clusters in the expansion.

In a recent letter, we reported $B_{2u} \leftarrow A_{1g}$ 6^1_0 spectra of $(C_6H_6)(C_6H_{12})_n$, $n = 1-10$.[25] Compared to the earlier study, clusters in the expansion were much colder: no broad baseline was observed in the smaller-size spectra, and reproducible sharp features were common throughout the sequence. The $n = 1-3$ spectra, dominated by vdW progressions, were analyzed to extract spectroscopic constants. Preliminary modeling computations were also reported, implemented on a single potential energy surface, with the limited aim of identifying reasonable structures that clarify interpretation of the spectra.

In this report, we begin a comprehensive computational study of the benzene−cyclohexane cluster system. Our computational strategy is elucidated in detail to provide transparency to the methodology and process. Application is made to the benzene−cyclohexane dimer, $(C_6H_6)(C_6H_{12})$, and trimer, $(C_6H_6)(C_6H_{12})_2$, to investigate several properties: low-temperature isomers, including their energies and optimized structures; average energies and structures at low temperature (2 K); and temperature-dependent phenomena, including rigid−nonrigid structural transitions. The trimer presents greater challenges than the dimer

* E-mail: easter@txstate.edu.

10.1021/jp045183g CCC: $30.25
Published on Web 01/08/2005

because of the coexistence of eight stable low-temperature isomers. Results are evaluated with reference to the R2PI spectra measured through benzene's 6^1_0 vibronic transition.[25]

II. Potential Energy Surfaces

Four different nonbonded pair potential energy functions are used in our $(C_6H_6)(C_6H_{12})_n$ simulations, originating from the work of Williams and Starr,[20] van de Waal,[16] Shi and Bartell,[23] and Jorgensen and Severance.[21] In previous modeling of neat benzene clusters, we adapted several authors' original interaction parameters to a common functional form

$$V_{ij}(r) = C_{\text{pre}} \exp(-C_{\text{exp}} r_{ij}) + C_{12} r_{ij}^{-12} + C_6 r_{ij}^{-6} + C_1 r_{ij}^{-1}$$

where r_{ij} is the distance between atoms i and j.[13,14] Using our adapted parameters, potential energies are calculated in units of kilojoules per mole. For neat benzene simulations, three separate sets of parameters are required, corresponding to each of the three interactions: C−C, C−H, and H−H. With benzene and cyclohexane molecules simultaneously present in the cluster, the original potential energy surface (PES) parameters must be adapted to include C_6H_{12}, which has unique bond lengths and partial atomic charges associated with its atoms. Potential energy parameters and their corresponding molecular bond distances are provided as Supporting Information to this report (Tables S1−S8). (Note that all Tables and Figures containing S in their identification label are located in the Supporting Information, e.g., Table S10, Figure S1.)

The main difference from the parameters tabulated in ref 14 is that we tabulate only the absolute value of C_1, specific to benzene−benzene interactions (Tables S1, S4, S5, and S7). $|C_1|$ is then multiplied by the appropriate factor (Table S2) to obtain the C_1 parameter for a given atom−atom interaction. This follows the approach of Williams and Starr.[20] Their original C_1 coefficients were based on the assumption that, for neutral hydrocarbons, hydrogen atoms can be assigned atomic charges, $q_H = (0.306\text{ e})/(n+1)$ where n represents the number of hydrogen atoms in the molecule's $-(CH_n)-$ groups.[16,20] For benzene, hydrogen's atomic charge is proportional to $^1/_2$ e ($n = 1$), whereas for cyclohexane, the charge is proportional to $^1/_3$ e ($n = 2$). Consequently, the hydrogenic charge in cyclohexane is two-thirds of the corresponding value in benzene. Molecular neutrality demands that the charge on the carbon atom be proportional to $-^1/_2$ e in benzene and to $-^2/_3$ e in cyclohexane. In Table S2, each of the four kinds of atoms is indicated in both the column and row headings, along with its relative charge. Tabulated entries are products of relative atomic charges; therefore, tabulated coefficients must be multiplied by the value of $|C_1|$ (C_6H_6) to obtain the appropriate C_1 coefficient for a given atom−atom interaction.

The Cartesian coordinates of five atoms in their *reference* orientations are also provided in Tables S3, S6, and S7. Because bond distances for cyclohexane were not available from refs 21 or 23, they were chosen to reflect the original authors' choice for benzene: distances are assumed to be standard for the Jorgensen potential; for the Shi and Bartell surface, the C−C bond is taken as standard, but the C−H bond is foreshortened to compensate for the asphericity of the hydrogen atoms.[23]

III. Coordinate Systems and Symmetry Considerations

III. A. Reference Orientations and Molecular Coordinates. *III. A. 1. Reference Orientations.* The reference (standard) orientations chosen for C_6H_6 and C_6H_{12} are shown in Figure 1. For both monomers, the z axis coincides with the molecule's highest-order rotation axis, with the $x-y$ plane being perpendicular to the principal axis. For the benzene molecule, the x axis is defined by two opposite carbon−hydrogen bonds. For cyclohexane, the x axis is defined by the line that intersects the molecular center, and the projections (on the $x-y$ plane) of two opposite carbon atoms; the *positive* x direction is assigned to the side of the molecule with the x axis carbon lying above the plane. Individual atoms in Figure 1 are assigned numbers for convenient reference.

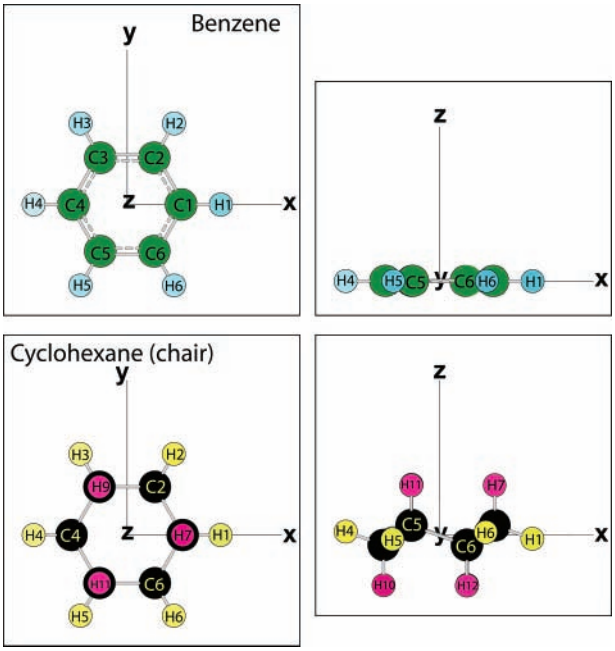

Figure 1. Reference (standard) orientations of the benzene (top row) and cyclohexane (bottom row) monomers. Both are viewed from the z axis (left column) and from the $-y$ axis (right column). Assignment of axes, numbering system, and color schemes are described in the narrative.

In both molecules, the atoms are numbered in a counterclockwise direction beginning with the atoms nearest the x axis. Thus, in benzene, C1 and H1 represent the carbon and hydrogen atoms lying on the x axis. In cyclohexane (*chair* configuration), C1, H1, and H7 represent the carbon atom, equatorial hydrogen atom, and axial hydrogen atom, respectively, whose projections fall on the $+x$ axis. H1−H6 are assigned to equatorial atoms, while H7 − H12 are assigned to axial atoms. The carbon and hydrogen atoms in benzene are dark green and light blue, respectively. For cyclohexane, the carbon, equatorial hydrogen, and axial hydrogen atoms are black, yellow, and pink, respectively.

To assign atomic Cartesian coordinates, it was assumed that benzene has D_{6h} symmetry and that cyclohexane (chair) belongs to the D_{3d} point group. Positions for C1 and H1 atoms in benzene were placed on the x axis at coordinates calculated from the PES bond distances. Coordinates of the other atoms were generated by successive application of the C_6 symmetry operation (described later). For cyclohexane, all bond angles were assumed to be tetrahedral. A nonlinear curve fit combines this assumption with the PES bond distances and the requirement that the x coordinate be zero to determine the coordinates of cyclohexane's C1, H1, and H7 atoms. Coordinates of the remaining atoms were generated by successive application of the S_6 symmetry operation (described later).

III. A. 2. Molecular Coordinates. Because the clusters under examination always contain exactly one benzene moiety, it is convenient to fix the benzene molecule's position and to equate

TABLE 1: Symmetry Operations for the D_{6h} (benzene) Point Group in Molecular Coordinates (see text)[a]

E	C_n^m	S_n^m	$(\sigma_{v,d})_n^m$	$(C_2')_n^m$
R	R	R	R	R
Θ	Θ	$\pi - \Theta$	Θ	$\pi - \Theta$
Φ	mod($\phi + 2m\pi/n$, 2π)	mod($\phi + 2m\pi/n$, 2π)	mod($2m\pi/n - \phi$, 2π)	mod($2m\pi/n - \phi$, 2π)
E/I	+1 (E)	−1 (I)	−1 (I)	+1 (E)
α	α	α	mod($\pi + \alpha$, 2π)	mod($\pi + \alpha$, 2π)
β	β	β	$\pi - \beta$	$\pi - \beta$
γ	mod($\gamma + 2m\pi/n$, 2π)	mod($\gamma + 2m\pi/n + \pi$, 2π)	mod($2m\pi/n + \pi - \gamma$, 2π)	mod($2m\pi/n - \gamma$, 2π)

[a] Molecular coordinates, initially (R, Θ, Φ, E/I, α, β, γ), will be transformed to the new molecular coordinates for the transformations identified in column headings. Symmetry operations in this table are applied with respect to the coordinate system origin and simultaneously affect all molecules in the cluster.

TABLE 2: Symmetry Transformations of Orientation Coordinates (E/I, α, β, γ) for an Individual Cyclohexane Molecule Located Somewhere Other than the Cluster Center[a]

E	C_n^m	S_n^m	$(\sigma_{v,d})_n^m$	$(C_2')_n^m$
E/I	E	I	I	E
α	mod($\alpha + 2m\pi/n$, 2π)	mod($\alpha + 2m\pi/n + \pi$, 2π)	mod($\pi - \alpha - 2m\pi/n$, 2π)	mod($-2m\pi/n - \alpha$, 2π)
β	β	β	$\pi - \beta$	$\pi - \beta$
γ	γ	γ	mod($\pi + \gamma$, 2π)	mod($\pi + \gamma$, 2π)

[a] The symmetry operation (column heading) is applied relative to the molecular center of mass. The center-of-mass coordinates (R, Θ, Φ) are unaffected by these transformations.

the cluster coordinate system with that of the reference benzene (Figure 1). The center of mass of each cyclohexane molecule is defined by a spherical polar coordinate triplet (R, Θ, Φ). The range of these coordinates is taken to be $0 \le R \le R_{max}$ (where R_{max} is set to 16 Å in the simulation), $0 \le \Theta < \pi$, and $0 \le \Phi < 2\pi$. Once the center-of-mass coordinates are established, all atomic coordinates of a cyclohexane molecule are unambiguously established by four additional coordinates. The first, E/I, indicates whether the molecule is in its identity state (E) or is inverted (I) before rotation about its center of mass. We define E/I = +1 for cases where the molecule is in its original orientation and E/I = −1 where inversion has been applied. The effect of E/I = −1 is to invert each atom through the molecular center of mass. Inclusion of the E/I coordinate is necessary to establish a self-contained set of symmetry operations for both the D_{6h} and D_{3d} point groups (Tables 1−2).

The remaining coordinates required to define atomic positions are three Euler angles, α, β, and γ, which describe the molecule's orientation about its center of mass (relative to the reference orientation). Transformation matrices describing the rotation of Cartesian coordinates are provided in the Supporting Information (Table S25).[26] From its standard (or inverted) orientation, the molecule is first rotated counterclockwise through an angle, α, about the z axis. The second rotation (β) is counterclockwise about the *original* y axis. The final rotation (γ) is analogous to the first, involving counterclockwise rotation about the *original* z axis. Ranges of the three Euler angles are taken to be $0 \le \alpha < 2\pi$, $0 \le \beta < \pi$, and $0 \le \gamma < 2\pi$.

One problem encountered when implementing range boundaries for angular coordinates is that predictable discontinuities occur. For Φ, α, and γ (range $0-2\pi$) the transformation between equivalent values is straightforward: when one of these parameters wanders outside a boundary, addition or subtraction of 2π brings it back into range. The corrections for Θ and β (range $0-\pi$) are less obvious, because simultaneous adjustments must be made to *more* than one variable. When Θ exceeds its limits ($\Theta \ge \pi$ or $\Theta < 0$), equivalencies are as follows: $\Theta + \pi$ (or $-\Theta$) $\rightarrow 2\pi - \Theta$ *and simultaneously* $\Phi \rightarrow \Phi + \pi$. When $\beta \ge \pi$ or $\beta < 0$, three simultaneous transformations are required: $\beta + \pi$ (or $-\beta$) $\rightarrow 2\pi - \beta$ *and* $\alpha \rightarrow \alpha + \pi$ *and* $\gamma \rightarrow \gamma + \pi$.

Each cyclohexane molecule in the cluster is uniquely described by a septet of molecular coordinates (R, Θ, Φ, E/I, α, β, γ). Application of the septet to an individual molecule first involves operation by the E/I coordinate, followed by rotation of the molecule through three Euler angles (α, β, γ) about its center of mass; the molecule is finally translated to its new center-of-mass coordinate (R, Θ, Φ). This coordinate system is economical in terms of the number of total coordinates and is well-suited for the application of symmetry operations (described later).

III. B. Symmetry Operations. Analysis of the reference orientations (Figure 1) reveals that the $3C_2$ and $3\sigma_d$ elements in D_{3d} are equivalent to the $3C_2''$ and $3\sigma_v$ elements in D_{6h}; equivalence of the remaining six D_{3d} symmetry elements is unambiguous.

In principle, a single isomer can be represented by a multitude of symmetry-equivalent coordinate sets. For example, when the benzene molecule defines the cluster's coordinate system, 24 distinct coordinate descriptions of the same isomer are generated via 24 D_{6h} operations. Furthermore, each *individual* cyclohexane molecule, operated on separately by 12 D_{3d} symmetry elements, gives rise to 12 distinct coordinate septets. Finally, because they are interchangeable, $n!$ ways exist of permuting n cyclohexane molecules. In total, for a $(C_6H_6)(C_6H_{12})_n$ cluster with n cyclohexane molecules, there exist $n!(24)(12)^n$ sets of n molecular coordinate septets that describe the same isomer. To identify and distinguish isomers, it is clearly necessary to analyze simulation results in light of symmetry.

III. B. 1. Symmetry Operations Relative to the Cluster (Benzene Molecule) Center. The 24 D_{6h} symmetry elements can be conveniently classified into 4 6-member groups, which we designate as C_n^m, S_n^m, $(\sigma_{v,d})_n^m$, and $(C_2')_n^m$. (1) The C_n^m operations involve rotation of the molecule by $2\pi m/n$ about its principal n-fold rotational axis. For benzene, $n = 6$ and $0 \le m \le 5$. Under D_{6h} symmetry, C_6^0 (our notation) = E (identity), $C_6^2 = C_3$, $C_6^3 = C_2$, and $C_6^4 = C_3^2$. (2) The S_n^m operations involve rotation of the molecule by $2\pi m/n$ about its principal axis, followed by reflection through the plane perpendicular to the principal axis. Equivalencies between our notation and common notation include $S_6^0 = \sigma_h$, $S_6^2 = S_3$, $S_6^3 = i$, and $S_6^4 = S_3^2$. (3) The $(\sigma_{v,d})_n^m$ operations involve reflection through a plane that is perpendicular to the principal ($x-y$, or σ_h) plane and intersects that plane at an angle of $m\pi/n$, measured counterclockwise from the x axis. Equivalencies in the D_{6h} point group include $(\sigma_{v,d})_6^{0,2,4} = 3\sigma_v$ and $(\sigma_{v,d})_6^{1,3,5} = 3\sigma_d$. (4) The

$(C_2')_n^m$ operations are characterized by a C_2 rotation about an axis that lies in the principal $(x-y)$ plane and is oriented at an angle of $m\pi/n$ measured clockwise from the x axis. In D_{6h}, $(C_2')_6^{0,2,4} = 3C_2'$ and $(C_2')_6^{1,3,5} = 3C_2''$. As noted previously, the D_{3d} point group consists of a 12-element subset of the D_{6h} group. The valid elements under D_{3d} symmetry correlate to our notation as follows: $C_6^{0,2,4} = E$, $2C^3$; $S_6^{1,3,5} = S_6$, i, S_6^5; $(\sigma_{v,d})_6^{0,2,4} = 3\sigma_d$; and $(C_2')_6^{1,3,5} = 3C_2$.

In Table S24, symmetry operations of the D_{6h} point group in Cartesian coordinates are collected. These transformations are applied relative to the origin of the coordinate system and simultaneously affect all coordinates in the system. Table 1 presents transformations for the same symmetry operations as *applied to our molecular coordinate system*. Each molecule in the cluster is simultaneously transformed by the application of these operations.

III. B. 2. Symmetry Operations Relative to a Cyclohexane Molecule's Center of Mass. The operations in Table 1 only partially address symmetry issues. Independent of operations applied to the entire cluster, each cyclohexane molecule can individually undergo twelve symmetry transformations *with respect to its own center of mass*. The application of D_{3d} symmetry operations to individual cyclohexane molecules is summarized by the molecular coordinate transformations in Table 2. Because they affect only the molecule's orientation, these transformations do not affect molecular center-of-mass coordinates.

III. C. Application of Symmetry to the Identification of Equivalent Structures. Each $(C_6H_6)(C_6H_{12})_n$ cluster is described by n molecular coordinate septets (R, Θ, Φ, E/I, α, β, γ). For a given structure, each of the $n!(24)12^n$ symmetry-equivalent coordinate sets can be generated through a nested application of symmetry operations. (1) In the outer loop, n cyclohexane molecules undergo $n!$ permutations. (2) In the first inner loop, the entire system is sequentially transformed through each of the 24 D_{6h} symmetry operations (Table 1). (3) In the n additional inner loops, each cyclohexane molecule is individually transformed through the D_{3d} symmetry operations (Table 2).

To ascertain whether a given set of coordinates represents a previously identified isomer, a "standard" set of coordinates is defined for the isomer. Given any set of coordinates, all symmetry-equivalent sets are generated and then evaluated against the standard coordinates. In our analysis, we have chosen to minimize the value of $\langle(\Delta r)^2\rangle$, which represents the mean-square distance between the standard and calculated Cartesian coordinates, averaged over *all* $18n$ cyclohexane *atoms* in the cluster.

IV. Computational Approach

IV. A. Monte Carlo Simulations. The computer code implemented to apply Metropolis Monte Carlo methodology[27] to benzene−cyclohexane clusters has been developed in our laboratory. The benzene molecule is held fixed in its reference orientation, and its molecular axes define the cluster coordinate system. Each cyclohexane molecule is described by six parametrized molecular coordinates (R, Θ, Φ, α, β, γ), with the seventh (E/I) set to $+1$. Each Monte Carlo step begins with the random selection of one of the n cyclohexane molecules in the cluster; its six molecular coordinates are independently modified to generate a test configuration. (Modification of each coordinate involves the random selection of a new coordinate within the range established by the coordinate's current *step size*.) The energy of the trial configuration is calculated and compared to that of the last accepted configuration, $\Delta\epsilon = \epsilon_{\text{last}} - \epsilon_{\text{test}}$. The value of the expression, $f = \exp(-\Delta\epsilon/kT)$, is evaluated and compared to a random number, r, where $0 < r < 1$. When $f > r$, the trial move is accepted, and the simulation proceeds from the new configuration; otherwise, the move is rejected, and the configuration reverts to the last accepted set of coordinates.

A typical simulation involves two nested cycles. The outer (temperature) cycle normally consists of 10^2-10^3 steps. The inner cycle consists of 10^4-10^5 isothermal Monte Carlo trial moves. Initial coordinate step sizes are estimated from standard deviations in previous simulations; step sizes are subsequently adjusted at the conclusion of each outer step to maintain an acceptance rate of $50 \pm 5\%$.

Several initial configurations are generated for each cluster size. For the dimer cluster, these consisted of a random assortment of cyclohexane positions and orientations. For larger clusters, initial configurations can be generated by randomly adding one molecule to the $n-1$ cluster structure. However, initial configurations have little effect on final structures in these studies, because the clusters are heated first to ensure randomization before the annealing process begins.

IV. B. Sequence of Computations. The computational sequence is carried out in five steps: generation of isomeric structures, identification of potential isomers, determination of minimum-energy structures, calculation of average cluster properties at low temperature, and monitoring the evolution of cluster properties as a function of temperature. For each of the five steps, independent sets of calculations are carried out on each of the four potential energy surfaces.

IV. B. 1. Step 1: Generation of Cluster Isomers. The initial structure is warmed (e.g., from 1 to 100 K). The cluster is then cooled in two steps: first, to its initial temperature (1 K), and subsequently, to very low temperature (e.g., 0.01 K). Five to ten initial configurations are used for each PES.

IV. B. 2. Step 2: Identification of Unique Isomers. Results from step 1 are analyzed to identify isomers. For each potential isomer, a standard set of coordinates is defined. Each configuration resulting from step 1 is evaluated on the basis of symmetry against each standard set of isomer coordinates. When the mean-square distance coefficient, $\langle(\Delta r^2)\rangle$, is less than 0.10 Å^2, isomeric equivalency is considered probable. A second metric for evaluating the equivalency of two structures run on the *same* PES involves the comparison of the cluster's total energy and its constituent molecules' stabilization energies. These must match if the structures are equivalent.

IV. B. 3. Step 3: Determination of Optimized Isomer Structures and Energies. The independent isomers identified in step 2 are established as initial configurations for simulated annealing calculations to low temperature. The resulting (optimized) structures are analyzed with reference to the original isomeric configuration to determine if the original (tentative) isomer occupies a local minimum on the PES. Coordinate and energy results are used to calculate average structures.

IV. B. 4. Step 4: Averages at Low Temperature. Each confirmed isomer surviving step 3 is used as a starting configuration in isothermal averaging simulations at low temperature (e.g., 2 K) to ascertain mean coordinates and energies and their standard deviations. Average cluster structures are analyzed with respect to the established isomers (step 3) to determine if their structures remain unique throughout the simulation. Typically, these simulations involve 10^3 isothermal outer cycles, each consisting of 10^4 Monte Carlo steps. Averages are calculated over only the last half of the isothermal cycles (i.e., after the system has equilibrated).

TABLE 3: Minimum Energy Isomer Coordinates and Energies for Each PES[a]

PES	R/Å	Θ	Φ	α	β	γ	E/kJ mol^{-1}	$\langle(\Delta r/\text{Å})^2\rangle$
Jorgensen	4.2285	0.3242	0.0004	6.2818	0.0183	0.0019	−12.3788	0.0132
Shi (3)	4.2336	0.3261	0.0011	5.8223	0.0011	0.4608	−11.1999	0.0131
van de Waal	4.3838	0.2848	6.2831	3.1323	0.0137	3.1512	−11.9572	0.0148
Williams	4.3302	0.2784	6.2831	3.1276	0.0194	3.1563	−11.9527	0.0135
mean value	4.2940	0.3034	0.0003	3.1502	0.0055	3.1333		
MP2/6-31g(d)	4.1566	0.2863	0.0001	3.1415	0.0557	3.1417	−8.23	0.0306

[a] Angles are in radians. The *mean* isomer molecular coordinates in the sixth row are constructed from the averaged *atomic Cartesian coordinates*. The last column indicates the mean-square atomic displacement for each individual structure, compared to the mean structure. In the last row, results from an MP2/6-31g(d) electronic structure calculation (section VI. A) are included for comparison; MP2 results were *not* used in the calculation of the mean structure.

IV. B. 5. Step 5: Temperature-Dependent Properties. The average structures (step 4) are used as initial configurations for caloric studies. As the structure is heated, its properties (e.g., its energy and positional coordinates) are monitored to assess temperature-dependent averages and standard deviations. Often, these data provide evidence of structural transitions.

V. Application to the Benzene−Cyclohexane Dimer: Results and Analysis

V. A. Generation and Identification of Isomers. Five starting dimer configurations were generated and run on each of the four PESs, for a total of 20 runs. Initial configurations were heated from 1 to 100 K to ensure randomization, cooled back to 1 K, and subsequently cooled further to 0.01 K. Each segment of the sequence (e.g., heating from 1 to 100 K) was carried out in 10^3 evenly spaced temperature steps, each consisting of 10^4 Monte Carlo trial moves.

The 20 resulting configurations were analyzed in terms of symmetry equivalency, as described in section III. C. For a given cyclohexane coordinate septet (R, Θ, Φ, E/I, α, β, γ), there exist a total of 287 other unique septets representing an equivalent structure. Following initial evaluation, a tentative standard coordinate septet was adopted for the dimer. Standard coordinates were arbitrarily chosen such that the cyclohexane moiety has a *positive z* center-of-mass coordinate and a near-zero x coordinate; it also has an orientation very close to that of the reference (Figure 1).

The parallel-displaced structure of the dimer, discussed in detail in the following text, contains Φ and β coordinates near zero, a situation requiring special care in analysis. ($\Phi = 0$ indicates that the molecular center of mass is on the x axis; $\beta = 0$ means that the molecule's principal plane is parallel to its standard orientation.) Near-zero coordinates in Φ and β give rise to two mathematical complications. For example, if two structures have identical coordinates, with the exception that one has $\Phi = 0.001$ and the other $\Phi = 6.282$, the two structures are a physical match, but their Φ coordinates are numerically different. The situation becomes more complicated when the difference is in the coordinate β (for example, when the two β values are 0.001 and −0.001). As discussed in section III. A. 2., when $\beta < 0$, the Euler coordinates (α, β, γ) transform to ($\alpha + \pi$, $-\beta$, $\gamma + \pi$), effecting discontinuities in *all three* Euler angles. To address this issue, molecular coordinate septets derived from the Monte Carlo simulations were used to generate Cartesian coordinates for the 18 cyclohexane atoms. For each structurally equivalent septet, a mean-square atomic displacement, $\langle(\Delta r^2)\rangle$, was calculated; the septet with the smallest $\langle(\Delta r^2)\rangle$ value was identified as the equivalent of the standard structure. A *single* isomeric structure was tentatively identified from analysis of all 20 initial simulations.

V. B. Dimer Structure and Energy Calculations. The standard structure of the tentative isomer was used as the initial configuration for four follow-up runs, each involving a different PES. For each, optimized coordinates and energies were determined by simulated annealing from 1 to 0.001 K, using 10^3 temperature steps, each consisting of 10^4 Monte Carlo steps. Results are collected in Table 3.

To determine the *mean* dimer structure coordinates, optimized molecular coordinates were not averaged directly; instead, molecular coordinates from each PES were used to calculate Cartesian coordinates of the *atomic* positions. Then, atomic Cartesian coordinates were averaged over the four PES structures, and results were converted back to molecular coordinates via a nonlinear fit. The mean values in Table 3 (row 6) represent the true average of the four PES structures in molecular coordinates. The value of $\langle(\Delta r^2)\rangle$ in the final column measures the mean-square displacement of atomic coordinates in the indicated PES structure, relative to the mean. These values are small, confirming that a single isomer is predicted by all four PES parameter sets.

For the dimer, an electronic structure calculation was carried out using the *Gaussian 03W*[28] package at the MP2/6-31g(d) level of theory (section VI. A.). Results are included in the last row of Table 3. The value of $\langle(\Delta r^2)\rangle$ (relative to the mean Monte Carlo structure) confirms that the MP2 and Monte Carlo structures are the same.

The mean structure resulting from the Monte Carlo studies is shown in Figure 2, presented from three different perspectives. The dimer structure is parallel-displaced. Cyclohexane's center of mass is located along the x axis ($X = 1.283$ Å, $Y = 0.000$ Å) and situated 4.098 Å above the benzene plane. Its molecular orientation is unchanged from the reference orientation: the tilt angle is extremely small ($\beta = 0.0055$ rad or 0.3°), and the sum, $\alpha + \gamma$, differs from 2π by 0.0003 rad (0.02°).

Relative positions of several cyclohexane atoms are worth noting. One axial hydrogen (H10) is directed to the center of the benzene ring; the other two axial atoms closest to benzene (H8 and H12) are directed halfway between two of benzene's hydrogen atoms. Of the three equatorial hydrogen atoms directly above the benzene ring, one rests above a benzene carbon (H4), while the other two are positioned midway between two of benzene hydrogens (H3 and H5). Of the four carbon atoms that reside above the benzene molecule, one is positioned above the center of the benzene ring (C4), two rest over benzene carbon atoms (C3 and C5), and the fourth sits above a hydrogen atom (C1).

V. C. Dimer Averages at 2 K. Independent isothermal simulations were run at 2 K on the 4 PESs to determine average structural coordinates and energies, along with their standard deviations. The simulations involved 10^3 isothermal cycles, each consisting of 2×10^4 Monte Carlo steps, but averaging was applied only over the final 500 isothermal cycles. The mean structure (Table 3 and Figure 2) was used as the initial configuration. To obtain meaningful averages, the normal range

TABLE 4: Results of the Isothermal Simulations at 2 K[a]

PES E_0 (kJ mol^{-1})	$\langle E\rangle$/kJ mol^{-1} $\langle E\rangle/E_0$ (%)	$S(E$/kJ mol$^{-1})$ $S(E)/E_0$ (%)	$\langle(\Delta r$/Å$)^2\rangle$	$E(A)$/kJ mol^{-1} $E(A)/E_0$ (%)
Jorgensen	−12.3150	0.6002	0.0067	−12.3717
−12.3788	99.48%	4.85%		99.94%
Shi	−11.1384	0.6062	0.0101	−11.1990
−11.1999	99.45%	5.41%		99.99%
van de Waal	−11.8932	0.6081	0.0163	−11.9482
−11.9572	99.46%	5.09%		99.92%
Williams	−11.8897	0.6004	0.0154	−11.9405
−11.9527	99.47%	5.02%		99.90%

[a]The left column identifies the PES and its minimum energy, E_0 (see Table 3). The second column contains the average energy; its standard deviation is in the third column. The fourth column contains the mean-squared coordinate displacement of the average structure, relative to the mean structure. In the last column is the theoretical energy associated with the thermally averaged structure. All percentage values are relative to E_0 for that PES.

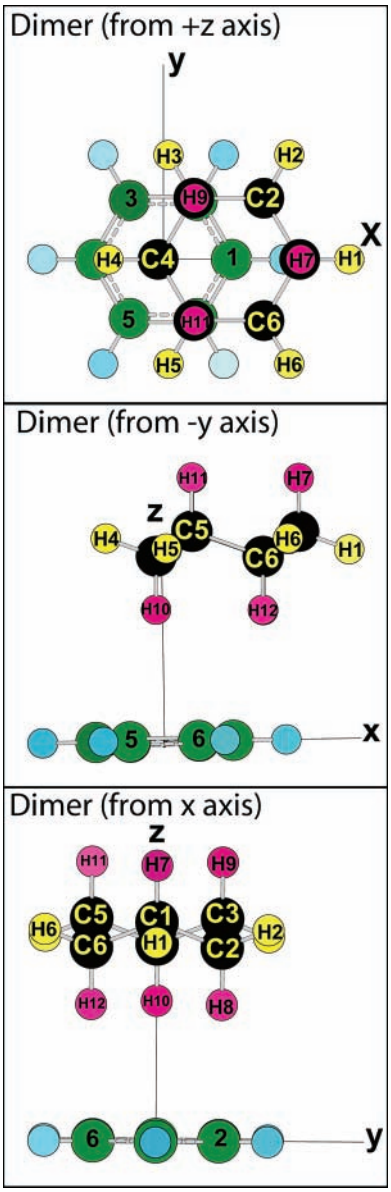

Figure 2. The average dimer structure, viewed from three perspectives: the $+z$ (top), $-y$ (middle), and $+x$ (bottom) axes. Atomic coloring is supplied to aid in distinguishing benzene's carbon and hydrogen (green, blue), and cyclohexane's carbon, equatorial hydrogen, and axial hydrogen (black, yellow, pink). Atomic numbering follows the convention established in Figure 1.

restrictions of the angular coordinates (Θ, Φ, α, β, γ) were lifted; averaged coordinates were not converted to standard-range values until the simulation was completed.

Table 4 contains the results from 2 K isothermal averaging. The first column identifies the potential energy surface and its respective minimum energy value (E_0) from Table 3. The second column contains the energy average (over 10^7 Monte Carlo steps), shown in units of kilojoules per mole and as a percentage of the minimum energy (E_0) for that PES. The third column contains the energy standard deviations. In the fourth column, the mean-square atomic coordinate displacement with respect to the mean structure is indicated. The fifth column lists the theoretical energy associated with the *average structure* for each PES.

Inspection of the data in Table 4 reveals noteworthy trends. The average configurational energy in 2 K isothermal simulations is consistently near 99.5% of the optimal energy, with standard deviations of ~5%. The small values of $\langle(\Delta r^2)\rangle$ indicate that thermal averages are a close reflection of the optimized structure. This is confirmed in that theoretical energies calculated from thermally averaged structures come within 0.1% of E_0 for each PES.

Standard deviations for molecular coordinates (R, Θ, Φ, α, β, γ) in 2 K simulations were 0.020 Å, 0.021, 0.052, 0.515, 0.024, 0.515, with angular coordinates in radians. A superficial look at the standard deviations of α and/or γ (~0.5) could lead to the erroneous conclusion that the molecule is fluxional at 2 K. To clarify the situation, it must be noted that the Euler coordinates, α and γ, become *mutually dependent* as β approaches zero. (In the specific case when $\beta = 0$, the molecule's counterclockwise rotation about the z axis is described by the *sum*, $\alpha + \gamma$, and any such rotation can be described by an infinite number of (α, γ) pairs.) The standard deviation of β (0.024) exceeds its mean value (0.0055, Table 3), implying that $\beta = 0$ for all practical purposes. To quantify the results, root-mean-squared standard deviations were calculated separately for Cartesian positions of the carbon, equatorial hydrogen, and axial hydrogen atoms, yielding values of 0.144, 0.188, and 0.147 Å, respectively. These small deviations in the atomic positions support the conclusion that the dimer is rigid at 2 K.

V. D. Caloric Curves for the Dimer. Two sets of simulations were carried out involving the heating of clusters while monitoring their energies and structures. Angular coordinate range limits were *not* enforced; coordinates from the previous cycle were converted to standard-range coordinates only at the conclusion of each temperature cycle. The first simulations employed all four PES parameter sets. These were run from 1 to 220 K in increments of +1 K; each temperature step consisted of 5×10^4 Monte Carlo Steps. The second set, run from 1 to 200 K, used only the Jorgensen PES. Increments of 0.1 K separated the temperature cycles, each of which consisted of 5×10^4 Monte Carlo Steps. To eliminate some of the noise in the latter data set, mean thermal energy values were smoothed

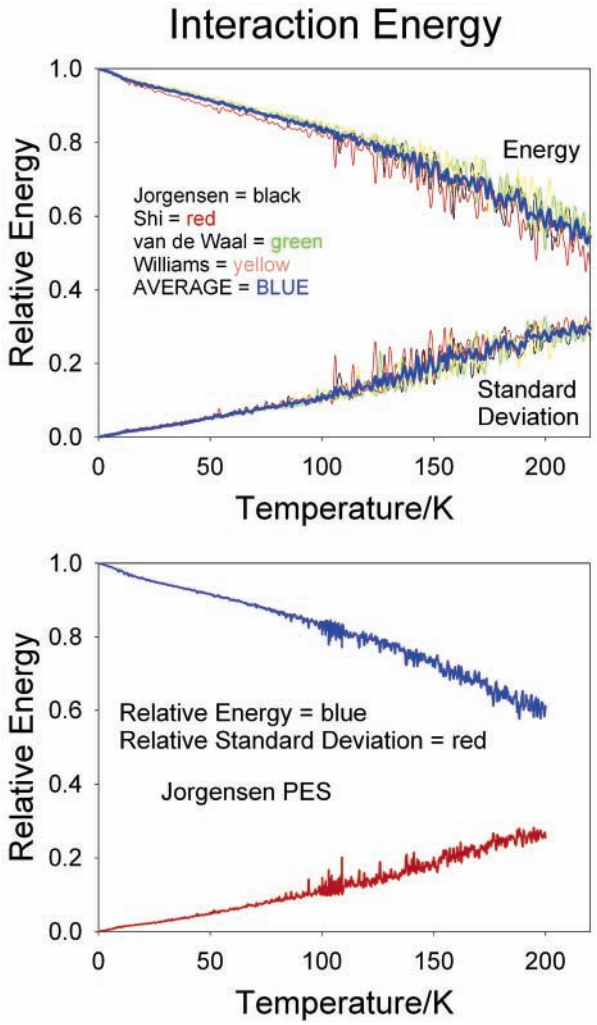

Figure 3. Configuration energy vs temperature. Each upper trace represents the relative energy; lower traces represent standard deviations. The top graph includes four PES results and their average (blue) at 1 K resolution. The lower graph has higher resolution (0.1 K before smoothing) from simulations using the Jorgensen PES.

by the relationship

$$E_S(T) = \frac{1}{2^n}\sum_{a=0}^{n}\frac{n!}{(a)!(n-a)!}E\left(T + s\left[a - \left(\frac{n}{2}\right)\right]\right)$$

where $E_S(T)$ is the smoothed energy value, $n = 8$ in our calculation, T is in K, and s is the increment between temperature steps in K ($s = 0.1$).

V. D. 1. Interaction Energy. The evolution of the mean interaction energy with temperature is shown in Figure 3, in which the energy and its standard deviation are both plotted versus the absolute temperature. The top figure contains "low-resolution" data from all four PES parameter sets; the *average* of the four is indicated by a bold blue trace. The lower figure shows the "high-resolution," smoothed results using the Jorgensen PES. For each PES, the energy scale is *relative* to its minimum value, E_0 (Table 3).

Predictably, favorable interaction energies decrease with increasing temperature, and their relative standard deviations increase. The energy plot changes slope (only slightly) at about 10 K; thereafter, it remains unchanged until about 100 K, where the fluctuation of values increases significantly. Comparison of the upper and lower halves of Figure 3 reveals no significant differences, suggesting that averaging low-resolution (1 K) caloric data over four distinct PES simulations can provide essentially the same information as a smoothed, high-resolution (0.1 K) simulation on a single PES.

V. D. 2. Positional Standard Deviations. In the caloric simulations, the standard deviations of cyclohexane's center-of-mass position and its constituent atomic positions (in Cartesian coordinates) were monitored. The dependence of these standard deviations on temperature is shown in Figure 4.

Each of the three graphs in Figure 4 consists of two plots: the lower plot represents the standard deviation of cyclohexane's center of mass; the upper plot traces the mean standard deviation of the atomic coordinates. The top graph includes data from the four PES simulations from 1 to 220 K; the middle graph contains the same data, expanded in the range from 1 to 100 K. The lower graph shows results from the smoothed, high-resolution simulations using the Jorgensen PES over the narrower temperature range.

Near 10 K, both plots show a sudden rise, indicating increased (through still constrained) motion of cyclohexane's center of mass, combined with freer rotational motion. Near 100 K, the plots in the top graph show an increase in slope, accompanied by a large increase in the magnitude of fluctuation. This is suggestive of much greater freedom of motion.

VI. Application to the Benzene−Cyclohexane Dimer: Discussion

VI. A. MP2 Calculations. It is intended that the computational strategy developed in this report be applicable to a broad range of cluster sizes. Because of computational resource requirements, electronic structure calculations are impractical for all except very small systems; as a result, they are not included in our "basic" strategy. Nevertheless, independent calculations on small clusters can be useful for confirming Monte Carlo results and for providing additional information that aids the interpretation of spectroscopic data.

For the dimer, we carried out optimization and frequency calculations at the MP2/6-31g(d) level of theory using *Gaussian 03* software.[28] To correct for known systematic errors, a scale factor (0.9676) was applied to resulting frequencies to calculate zero-point corrections.[29] The mean structure (Table 3) was used as the initial dimer configuration. Additional calculations were run on the benzene and cyclohexane monomers to obtain electronic and zero-point energies.

The optimized MP2 structure was transformed to our molecular coordinate system. The results are included in the bottom row of Table 3. Inspection of the resulting coordinates reveals close agreement with the mean Monte Carlo structure. This assessment is confirmed quantitatively by the small mean-square displacement value, $\langle(\Delta r)^2\rangle = 0.0306$ Å^2.

Table 5 includes the MP2 energy data. The first three energies shown in the table indicate the sum of the electronic energy and the zero-point energy correction. The fourth entry represents the difference between product and reactant energies, corresponding to the dimerization process, $C_6H_6 + C_6H_{12} \rightarrow (C_6H_6)$-$(C_6H_{12})$. The net energy of dimerization is calculated to be -8.23 kJ mol^{-1} at low temperature (T), which is within ~4 kJ mol^{-1} of the Monte Carlo interaction energies predicted by the four empirical PES parameter sets.

MP2 frequency calculations identified six vdW modes. In Table 6, the modes are listed in order of increasing energy; fundamental wavenumbers (cm^{-1}) are shown in the right column. Four varieties of molecular motion are observed in the modes. (1) *Twist*: small-amplitude rotational oscillation of a molecule about its principal rotation (z) axis. (2) *Seesaw (axis)*: The principal molecular plane rocks up and down as if

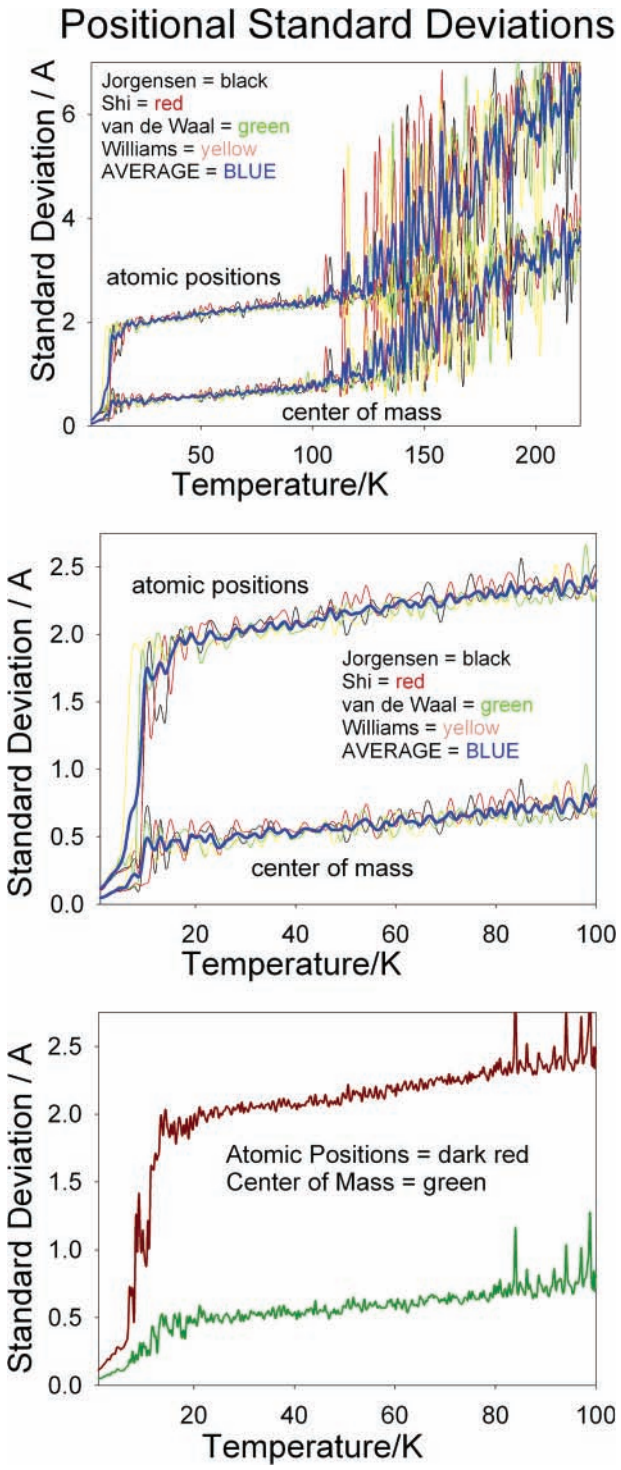

Figure 4. Positional standard deviations vs temperature. The lower trace of each plot represents the standard deviation of cyclohexane's center of mass; the upper trace represents the mean atomic standard deviation. Results for all four PESs (and their average) are plotted (top) to 220 K; the center graph contains the same data from 1 to 100 K. The bottom graph contains corresponding data for the high-resolution simulation based on the Jorgensen PES.

it were a seesaw, with the axis acting as a fulcrum identified in parentheses. (3) *Fan (atom, axis)*: The molecule's principal plane waves like a fan. The atom and axis (in parentheses) identify the atom that remains stationary and the molecular axis that is collinear with the fan's "handle". (4) *Stretch*: The entire molecule undergoes small oscillations in the *z* direction; the orientation of the principal plane is unchanged. Additional notation used in Table 6 includes the following: B and C represent benzene and cyclohexane, respectively; L and S represent large- and small-amplitude displacements (when there is a difference between the molecules). Finally, simultaneous motions of the benzene and cyclohexane moieties can occur either in the same or in opposite directions. The results shown in Table 6 are discussed further in section VI. C.

TABLE 5: MP2 Energies Calculated for the Two Monomers and the Dimer[a]

MP2/6-31g(d)	energy (hartrees)
C_6H_6	−231.362 893
C_6H_{12}	−234.823 089
$(C_6H_6)(C_6H_{12})$	−466.189 118
difference	−0.003 136
difference: kJ mol^{-1}	−8.23

[a] All entries except the last are in hartrees. Entries for each species represent the sum of the electronic energy and the zero-point correction.

TABLE 6: MP2/6-31g(d) van der Waals Fundamentals (in cm^{-1}) for the Dimer[a]

no.	description	fundamental
1	B: twist C: twist in the opposite direction.	11.6
2	B: seesaw (*x*-axis), S C: seesaw (*x*-axis), L, in the opposite direction.	33.4
3	B: seesaw (*y*-axis), S C: seesaw (*y*-axis), L, in the same direction.	37.1
4	B: seesaw (*y*-axis), L C: seesaw (*y*-axis), S, in the opposite direction.	61.8
5	B: Seesaw (*x*-axis), L C: seesaw (*x*-axis), S, in the same direction.	62.1
6	B: fan (H4, *x*-axis) C: stretch in the same direction.	65.5

[a] Terms and other notation used in the descriptions are defined in the text.

VI. B. Isomers and Structures. The results of this study (based on Monte Carlo simulations using four different potential energy surfaces) point to a conclusion that is confirmed by MP2 electronic structure calculations: there is a single minimum-energy dimer isomer. The structure is parallel-displaced, with the cyclohexane moiety's center of mass positioned 4.10 Å above the benzene axis and displaced 1.28 Å in the *x* direction. The averaged structure in isothermal simulations at 2 K is unchanged from the optimized structure. This implies that experimental measurements on dimers in cold supersonic expansions, which show reproducible sharp spectral features, are effectively measuring properties of the dimer's optimal structure.[25]

VI. C. Relationship to Experimental Results. The dimer's resonance-enhanced two-photon one-color UV spectrum has been previously reported, as measured through benzene's $B_{2u} \leftarrow A_{1g}$ 6^1_0 transition near 260 nm.[25] Although the raw spectrum contained fragmentation artifacts originating from the trimer, the application of spectral subtraction techniques successfully removed all except one fragmentation feature, resulting in the corrected dimer spectrum shown in Figure 5.

To interpret the van der Waals progression, term values are assigned to electronic vibrational states in the form

$$T(n, \upsilon) = \bar{\nu}(n) + \bar{\nu}_e\left(\upsilon + \frac{1}{2}\right) - \bar{\nu}_e\chi_e\left(\upsilon + \frac{1}{2}\right)^2$$

where T is the term value (in reciprocal centimeters), $\bar{\nu}(n)$ represents the energy minimum of the electronic PES, $\bar{\nu}_e$ is the fundamental wavenumber, and $\bar{\nu}_e\chi_e$ is the anharmonicity constant. The values n and υ represent the electronic and vibrational

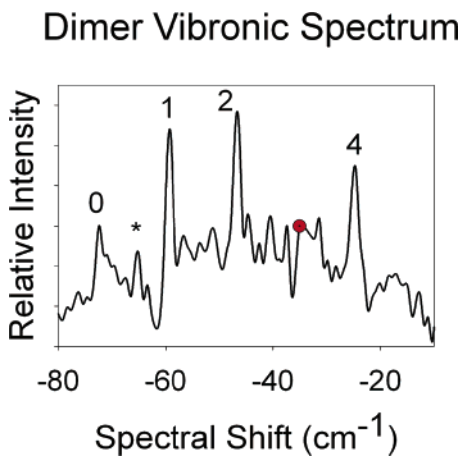

Figure 5. Vibronic spectrum of the dimer from ref 25. Features are identified by upper-state vdW vibrational quantum number, υ'. The asterisk indicates a feature resulting from fragmentation of the trimer. The calculated position of the $\upsilon' = 3$ feature (-35 cm^{-1}) is identified by a circle.

quantum numbers, respectively. The transition wavenumber is the difference between the upper- and lower-state term values, $T(n', \upsilon') - T(n'', \upsilon'')$. Assuming that the vdW modes are in their zero-point levels ($\upsilon'' = 0$) in the ground electronic state and that the vdW frequencies are the same in both electronic states, we can reduce the transition wavenumber to the relationship

$$\bar{\nu} \approx \bar{\nu}_0 + \bar{\nu}_e(\upsilon') - \bar{\nu}_e\chi_e(\upsilon'^2 + \upsilon')$$

where $\bar{\nu}_0$ equals $\bar{\nu}(n') - \bar{\nu}(n'')$ and represents the 0−0 transition origin. We report both $\bar{\nu}$ and $\bar{\nu}_0$ as shifts relative to the molecular benzene 6_1^0 transition (38 608.1 cm^{-1}).

Four features are prominent in the dimer spectrum, characterized by spectral shifts of -72.4, -59.0, -47.0, and -24.6 cm^{-1}. (An asterisk in the spectrum identifies a fragmentation feature originating from the trimer cluster.) The data are consistent with a van der Waals progression having the following spectroscopic constants: $\bar{\nu}_0 = -72.3 \pm 0.3$ cm^{-1}, $\bar{\nu}_e = 13.9 \pm 0.4$ cm^{-1}, and $\bar{\nu}_e\chi_e = 0.40 \pm 0.08$ cm^{-1}. Features predicted from these constants fall within 0.2 cm^{-1} of experimentally observed transitions, well within the experimental resolution of ~0.75 cm^{-1}. Relative intensities increase from $\upsilon' = 0$ to a maximum at $\upsilon' = 2$ and decrease thereafter. The calculated feature for the $\upsilon' = 3$ feature (-35 cm^{-1}) is either absent or has low intensity; its calculated position is marked by a circle in Figure 5.

Schlag and co-workers reported a single broad feature for the BC_1 dimer, with a spectral shift of -47.2 cm^{-1};[1] El-Shall and Whetten reported a similar feature in their study.[24] This shift corresponds to the $\upsilon' = 2$ level of the vdW mode (-47.0 cm^{-1}), the most intense feature. The intensity pattern suggests relaxation along this mode's coordinate in the excited state. It is not surprising that the most intense vdW transition was the one previously observed in experiments involving warmer $(C_6H_6)(C_6H_{12})$ expansions.

Nonlinear molecules are characterized by $3N$ degrees of freedom: 3 translational, 3 rotational, and $3N - 6$ vibrational degrees, where N is the number of atoms in the molecule. There are 30 vibrational modes for C_6H_6 and 48 for C_6H_{12}. When n cyclohexane molecules are combined with one benzene molecule to form a $(C_6H_6)(C_6H_{12})_n$ cluster, $3n$ translational and $3n$ rotational modes are lost, compared to the total number for the separated molecules. When molecular vibrational modes are distinct and well-separated from the vdW modes, this gives rise to $6n$ vdW modes.

As expected, six vdW modes were identified by MP2 calculations (section VI. A.). Of the six, only one has a fundamental wavenumber close to the experimental value of ~14 cm^{-1}. If the MP2 frequency results are correct, the vdW mode observed in the R2PI spectrum corresponds to the lowest-energy MP2 mode (~12 cm^{-1}), which consists of simultaneous twisting (in opposite directions) of the benzene and cyclohexane molecules; while they twist, the principal molecular planes remain parallel.

VI. D. Structural Transitions from Rigid to Nonrigid. The caloric studies identify two temperatures at which a structural transition may occur. At or below 10 K, the energy versus temperature plot changes slope, though only slightly. More obvious in this temperature range is the increase of standard deviations for both the center-of-mass and the mean atomic coordinates. These trends are consistent with the transition from a completely rigid cluster to one in which the cyclohexane molecule has much greater freedom to rotate about its principal axis, accompanied by limited mobility of its center of mass.

A second change, near 100 K, is marked by increased scatter (both in the average energy and positional standard deviation data) with the slope of the standard deviation versus temperature plots increasing noticeably. The data above 100 K are consistent with a fluxional dimer in which the constituent molecules enjoy much greater translational and rotation freedom. It should be noted, however, that the data do not appear to indicate dissociation at temperatures below 220 K, where the average configurational energy is still within 50% of the optimum value, and standard deviations of the cyclohexane center-of-mass coordinates are less than 4 Å, compared to the imposed center-of-mass coordinate limit, $R_{max} = 16$ Å.

If these inferences are correct, the dimer exists in three distinct forms in the range from 1 to 220 K. At very low temperatures (<10 K), the structure is rigid. In the intermediate range ($10 < T < 100$ K), cyclohexane's center of mass remains fairly immobile, while molecular rotation is freed. In the higher temperature range ($100 < T < 220$ K), both translational and rotational motions are less restricted; however, the dimer remains bound, while the interaction energy becomes less favorable as temperature increases. The sharp, reproducible features in the vibronic spectrum (Figure 5) imply that dimer clusters in that experiment's supersonic expansion were rigid, with a translational temperature below 10 K.

VII. Application to the Trimer, $(C_6H_6)(C_6H_{12})_2$: Results and Analysis.

VII. A. Trimer Calculations. Computations on the trimer were carried out through a sequence of Monte Carlo calculations, run separately on all 4 PESs: (1) Six different starting configurations were randomly generated and heated from 1 to 100 K. (All simulations here, and in step 3, used 10^3 evenly spaced temperature (T) steps, each consisting of 10^4 Monte Carlo (MC) trial moves.) Resulting configurations were cooled back to 1 K and subsequently cooled further to 0.01 K. (2) The 24 resulting structures (6 initial configurations × 4 PESs) were analyzed for symmetry equivalency, with 8 potential isomers being identified. (3) Each of the 8 potential configurations was cooled from 1 to 0.001 K to determine if the isomer occupies a relative minimum position on the 4 PESs and to define its optimal coordinates. For each isomer, the *mean* molecular coordinates (referred to as the standard) were calculated from the *atomic* Cartesian positions, averaged over the 4 PES results. The result from each PES was compared to the standard by calculating a mean-square distance coefficient, $\langle(\Delta r)^2\rangle$, quantify-

TABLE 7: Molecular Coordinates (columns) for Sandwich 1 Isomer[a]

sandwich **1** (S_3)	C_6H_{12}	R (Å)	Θ	Φ	E/I	α	β	γ
Jorgensen	1	4.2226	0.3247	0.0163	1	6.0260	0.0188	0.2604
	2	4.2228	2.8166	2.0798	−1	0.1211	0.0188	5.1093
Shi (3)	1	4.2273	0.3253	0.0134	1	4.6897	0.0041	1.5974
	2	4.2277	2.8143	2.0837	−1	0.5682	0.0028	4.6630
van de Waal	1	4.3773	0.2848	0.0136	1	3.3820	0.0139	2.9038
	2	4.3774	2.8568	2.0810	−1	2.9047	0.0138	2.3271
Williams	1	4.3228	0.2787	0.0176	1	3.4154	0.0201	2.8699
	2	4.3230	2.8631	2.0774	−1	2.9452	0.0195	2.2881
mean value								
	1	4.2876	0.3036	0.0004	1	3.1504	0.0048	3.1326
	2	4.2876	2.8380	2.0948	−1	3.1504	0.0048	2.0854

[a] Results are shown for each of the four PESs. The mean values of the Euler angles are based on *atomic positions*, and are not the direct average of four PES values. Distances are in angstroms, and angles are in radians.

TABLE 8: Key Results for Sandwich 1 Isomer[a]

trimer sandwich **1** (S_3)	Jorgensen	Shi (3)	van de Waal	Williams
E (kJ mol^{-1})	−25.2694	−22.8550	−24.4115	−24.3910
$\langle(\Delta r)^2\rangle$/Å^2 (opt)	0.0142	0.0134	0.0152	0.0138
%E (C_6H_6)	48.98%	49.00%	48.98%	49.00%
%E (C_6H_{12} #1)	25.51%	25.50%	25.51%	25.50%
%E (C_6H_{12} #2)	25.51%	25.50%	25.51%	25.50%
$\langle(\Delta r)^2\rangle$/Å^2 (2 K avg structure)	0.0071	0.0105	0.0171	0.0158
%E (2 K avg structure)	99.91%	99.99%	99.93%	99.92%
%$\langle E\rangle$ (2 K)	99.56%	99.53%	99.55%	99.54%
%$\sigma(E)$ (2 K)	2.82%	3.11%	2.90%	2.86%
$\sigma(r)$/Å (2 K)	0.1298	0.1293	0.1455	0.1588

[a] Results are shown for each of the four PESs (column headings) used in this study. Row 2 contains the optimized energy (kJ mol^{-1}). Row 3 shows the mean-squared displacement of each PES result relative to the mean structure. Rows 4−6 indicate the distribution of interaction stabilization among the three molecules. Rows 7−8 contain the mean-squared displacement of the thermally averaged structure (2 K) and its energy relative to the optimized structure. Rows 9−11 tabulate the average energy and its standard deviation in 2 K simulations and the standard deviation of cyclohexane's 36 atomic positions.

ing the square of the difference in the position between the PES optimum structure and the standard structure, averaged over all 36 cyclohexane atoms. In most cases, the value of $\langle(\Delta r)^2\rangle$ is less than 0.02 Å^2; in all cases except one (discussed later), the value is less than 0.05 Å^2, indicating a uniformity in the 4 PES predictions. (4) Isothermal simulations were run for each of the 8 isomers at 2 K to determine mean structural coordinates (and standard deviations) and to ascertain whether the isomers maintain unique structures at low temperature. The latter simulations involved 1000 isothermal steps, each consisting of 2×10^4 trial moves. Averaging was applied only over the final 500 isothermal cycles (i.e., 10^7 trial moves). 5. Temperature dependence was investigated by heating each isomer from 1 to 110 K in 1 K steps, each isothermal step consisting of 5×10^4 trial moves. The cluster's interaction energy was monitored, as were coordinates of the atomic positions and centers of mass.

VII. B. Trimer Isomers. The eight trimer isomers fall into two general classifications. Three isomers can be described as *sandwich* structures, wherein the two cyclohexane molecules constitute the "bread" of a benzene sandwich. The principal planes of the cyclohexane molecules are essentially parallel to that of benzene; the cyclohexane molecules are equivalent, being mutually related through a D_{6h} symmetry operation. Molecular coordinates are arbitrarily defined such that molecule **1** has a positive z center-of-mass coordinate that lies close to the x axis; its rotational coordinates are chosen to mimic those of the standard molecular configuration. Each of the three sandwich structures can be viewed as constructed by direct addition to the (C_6H_6)(C_6H_{12}) dimer (Figure 2), with the additional C_6H_{12} molecule effecting minimal change to the coordinates of the original dimer molecules. Of the two classes, the sandwich structures have the least favorable interaction energies. Nearly half of the cluster's interaction energy is associated with the benzene moiety, with the remainder equally split between cyclohexane molecules.

The remaining five isomers are classified as *trigonal*. These structures contain two nonparallel cyclohexane molecules unrelated by symmetry. The molecule with the greatest $|z|$ coordinate is designated as molecule **1** and is loosely referred to as *axial*; the remaining cyclohexane (molecule **2**) is designated *equatorial*. These labels, axial and equatorial, are approximations and neither imply that one cyclohexane center of mass falls on the cluster z axis nor that the other lies in the $x-y$ plane. All five trigonal isomers are lower in energy than the sandwich structures. Of the constituent molecules, the axial cyclohexane is always associated with the most favorable stabilization interactions. Molecular coordinates of molecule **1** are arbitrarily chosen such that the center of mass has a positive z coordinate and is near the x axis; its β coordinate is restricted to the range $0 \le \beta < \pi$. For both cyclohexane moieties, we have chosen E/I = +1. The choice of the other two Euler angles, α and γ, is arbitrary. The isomer numbers (e.g., sandwich **3**, trigonal **2**) are also arbitrary.

*VII. B. 1. Sandwich **1** (S_3).* The sandwich **1** isomer consists of two cyclohexane molecules related by S_3 symmetry, occupying positions on opposite sides of the C_6H_6 plane. Quantitative results are summarized in Tables 7−8. Table 7 contains optimized molecular coordinates (column headings) for each of the four PESs identified in the left column. Distance coordinates are in angstroms, and angular coordinates are in radians. The coordinates of molecules **1** and **2** reflect S_3 symmetry. It is important to note that the mean molecular coordinates (last two rows) are *not* determined via a simple average of Euler coordinates from the four PES computational results. As for the dimer, direct averaging of the Euler coordinates is unreliable when one or more cyclohexane

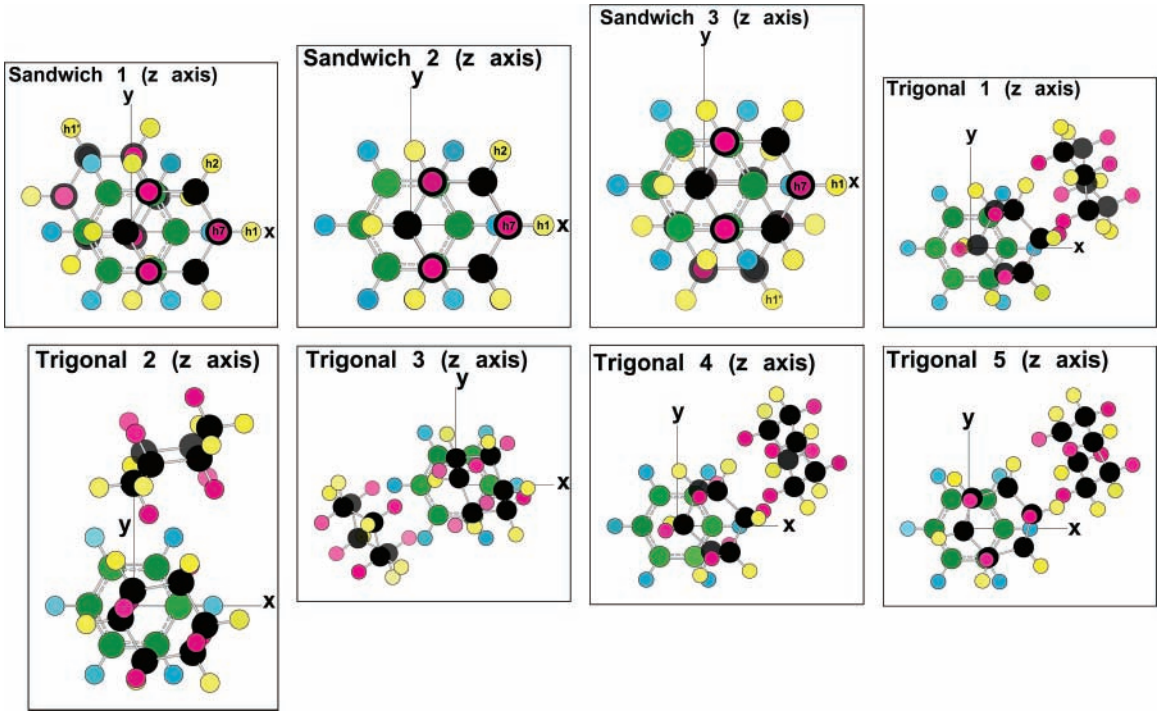

Figure 6. View of each of the trimer isomers from the $+z$ axis. A few hydrogen atoms are labeled to emphasize symmetry in the sandwich isomers; the cyclohexane molecules are inequivalent in the trigonal isomers. As a visual aid, benzene's C and H atoms are green and blue, respectively; cyclohexane's C, equatorial H, and axial H atoms are black, yellow, and pink, respectively. The same color scheme is used in subsequent figures.

molecules are parallel to the cluster's $x-y$ plane. To address this issue, all C_6H_{12} atomic coordinates are first averaged over the four PES results, with the results being converted to molecular coordinates via a nonlinear fit. This approach was adopted for all eight isomers in this study (even for the trigonal isomers where direct averaging would have been satisfactory). Tables analogous to Table 7 for the other isomers are arranged identically and can be found in the Supporting Information (Tables S9−S13 and S15−S16).

Key results for the sandwich **1** isomer are presented in Table 8 for the PESs (column headings). Row 2 contains the isomer's optimized energy in kilojoules per mole. Row 3 gives the mean-square displacement value, $\langle(\Delta r)^2\rangle$ in units of Å^2, indicating the degree of agreement between individual PES results and the mean value. Note that no value is greater than 0.0152 Å^2, indicating excellent agreement. Rows 4−6 show the percentage of the cluster's stabilization energy associated with each molecule: 49.0% is localized on the benzene molecule, with the remainder split equally between cyclohexanes. Rows 7−8 tabulate the mean-squared distance and the theoretical energy of the thermally averaged structure at 2 K. For sandwich **1**, values of $\langle(\Delta r)^2\rangle$ for the thermal averages mimic those of the optimized structures, and their energies fall within 0.1% of the optima, confirming that the isomer is unique and occupies a local energy minimum at 2 K. Rows 9−11 contain the average energy at 2 K ($\langle E\rangle$), along with its standard deviation ($\sigma(E)$), and the positional standard deviation of cyclohexane's 36 atomic coordinates ($\sigma(r)$). These data further attest to the isomer's uniqueness at low temperature. Analogous tables containing key results for the remaining 7 isomers are identically arranged and are collected in the Supporting Information (Tables S17−S23).

The structure of the sandwich **1** isomer is shown in Figures 6, 7, and S1 (top left corner). Figure 6 compares all eight isomers from the perspective of the z axis; The same structures are compared from the $-y$ axis in Figure 7, and from the x axis in Figure S1. A subset of the hydrogen molecules are labeled to emphasize the S_3 relationship between cyclohexane moieties. The upper molecule (molecule **1**) has a position and orientation essentially identical to its counterpart in the dimer cluster. The same is true for all three sandwich structures, which differ from each other only in the placement and orientation of molecule **2**. The three sandwich structures have higher energies than the trigonal isomers, and sandwich **1** has the highest energy of the three.

*VII. B. 2. Sandwich **2** (σ_h).* The sandwich **2** isomer has its cyclohexane members related by σ_h symmetry, occupying opposite sides of the benzene plane. The substantive difference from the sandwich **1** structure lies in the position and orientation of the second cyclohexane molecule. Quantitative results are summarized in Tables S9 and S17, and the mean optimized structure is shown in Figures 6, 7, and S1. Mean-square displacement values for the optimized PES results versus the mean structure are $\leq$0.0154 Å^2, demonstrating strong agreement between individual PES results. The percentage of the cluster's stabilization energy associated with benzene is ∼48.8%; the rest is shared equally between the two C_6H_{12} molecules. Mean-squared displacements ($\leq$0.0182 Å^2) and relative theoretical energies of the thermally averaged structures at 2 K ($\geq$98.4%) suggest that the optimal structure is well approximated by thermal averages at 2 K. This is supported by the calculated average 2 K energies, which are ∼99.5% of the optimum. Comparison of the two isomers in Figures 6, 7, and S1 confirms that the difference between the sandwich **1** and **2** structures is in the position and orientation of the $C_6H_{12}-2$ molecule. Of the three sandwich isomers, sandwich **2** is lowest in energy.

*VII. B. 3. Sandwich **3** (S_6^5).* The sandwich **3** isomer has two cyclohexane molecules related by S_6^5 symmetry, occupying opposite sides of the benzene plane. Like sandwich **2**, the key difference from sandwich **1** lies in the position and orientation of the second cyclohexane molecule, as seen in Figures 6, 7, and S1. Quantitative results are summarized in Tables S10 and S18. Mean-square displacement values for the optimized PES results versus the mean are $\leq$0.0162 Å^2, reflecting solid agreement among PES results. The percentage of the cluster's stabilization energy associated with benzene is ∼48.9%, with

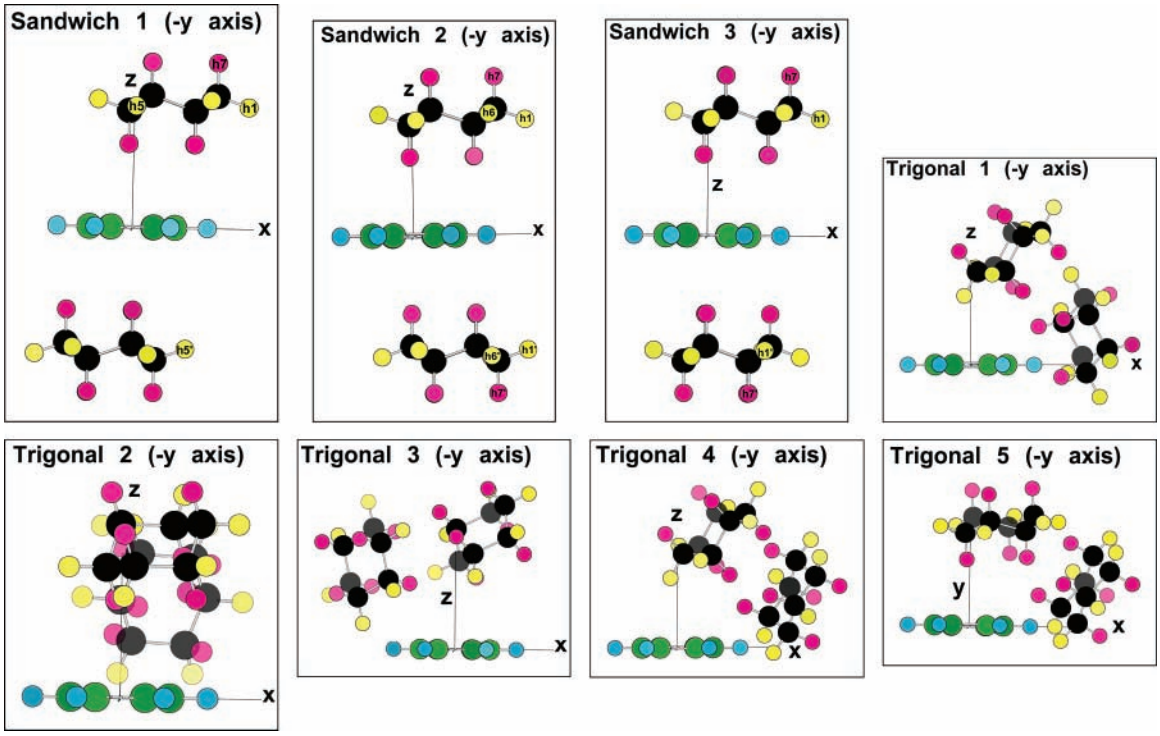

Figure 7. View of each of the trimer isomers from the $-y$ axis. The cyclohexane molecules are related by symmetry in the sandwich isomers, but are inequivalent in the trigonal isomers.

the remainder equally split between C_6H_{12} moieties. The mean-squared displacements (≤ 0.0177 Å^2) and the relative theoretical energies of the thermally averaged structures at 2 K ($\sim$99.9%) indicate equivalence between the 2 K thermal average and the optimized structure. The mean energy at 2 K is $\sim$99.5% of the optimum. Of the three sandwich isomers, sandwich **3** is intermediate in energy.

*VII. B. 4. Trigonal **1***. The structure of the trigonal **1** isomer is shown in Figures 6, 7, and S1. Quantitative results are collected in Tables S11 and S19. In comparison to the sandwich isomers, all trigonal isomers have lower energy. Within this class of isomers, the two cyclohexane molecules are distinct, with the axial member (i.e., the one having the greatest $|z|$ center-of-mass coordinate) experiencing the greatest stabilization energy. The cluster's total interaction energy is distributed among C_6H_6, $C_6H_{12}-1$, and $C_6H_{12}-2$ in the percentages 33%, 37%, and 30%. The axial cyclohexane molecule is located 4.739 Å from the coordinate system origin, with center-of-mass (CM) coordinates of (1.500, 0.226, 4.490) Å, and a tilt of 41.6°. Its equatorial counterpart is centered at 5.520 Å from the origin, with CM coordinates of (4.619, 2.793, 1.154) Å and a molecular tilt of 98.3°. Both centers of mass reside above benzene's molecular plane, a characteristic common to all five trigonal isomers. Quantitative results in Table S19 confirm that the structure is unique at $T = 2$ K.

*VII. B. 5. Trigonal **2***. The structure of the trigonal **2** isomer is shown in Figures 6, 7, and S1. Quantitative results are collected in Tables S12 and S20. The cluster's total interaction energy is distributed among C_6H_6, $C_6H_{12}-1$, and $C_6H_{12}-2$ in the approximate percentages 34%, 37%, and 29%. The axial cyclohexane molecule is located 4.455 Å from the coordinate system origin, with CM coordinates of (0.902, -0.493, 4.335) Å and a tilt of 33.4°. Its equatorial counterpart is centered at 5.605 Å from the origin, with CM coordinates of (1.177, 4.706, 2.807) Å and a molecular tilt of 99.7°. Both centers of mass lie above benzene's molecular plane. Quantitative results in Table S20 indicate that that the structure is unique at 2 K.

*VII. B. 6. Trigonal **3***. The mean structure of the trigonal **3** isomer is shown in Figures 6, 7, and S1. Quantitative results are collected in Tables S13, S14, and S21. For the other seven trimer isomers, there is remarkable agreement between structures independently predicted by four PESs. The trigonal **3** trimer presents the lone exception. Simulated annealing calculations carried out to determine optimal coordinates (starting with the standard isomer coordinates) identify similar structures for all four PESs, with the results collected in Table S13. However, when subjected to isothermal averaging at 2 K, a somewhat different (lower-energy) structure is identified, but only on the Williams PES. Annealing of the unique Williams structure to very low temperature yields the structural coordinates collected in Table S14. It is apparent that the Williams PES has two adjacent local minima: the first, which agrees with the structure predicted by the other three PESs, is extremely shallow; the second has lower energy and is easily accessed from the first in simulations at 2 K. The calculated value, $\langle(\Delta r)^2\rangle = 1.27$ Å^2, confirms that the lower-energy Williams trigonal **3** structure is different from the others.

Coordinates in Table S13 reflect the higher-energy structure for the Williams PES, and isomer averages are based on those values. Values in Table S21, however, reflect the lower-energy structure; the affected values are identified with an asterisk. The total interaction energy is distributed among C_6H_6, $C_6H_{12}-1$, and $C_6H_{12}-2$ in the approximate percentages $32^1/_2$%, 36%, and $31^1/_2$%. The axial cyclohexane molecule is located 4.852 Å from the coordinate system origin, with CM coordinates of (1.161, 0.031, 4.711) Å and a tilt of 52.2°. Its equatorial counterpart is centered at 5.382 Å from the origin, with CM coordinates of (-4.003, -0.763, 3.516) Å and a molecular tilt of 98.1°. Both centers of mass lie above benzene's molecular plane. They are, however, located on opposite ends of the benzene hexagon, an exception to the pattern of the other trigonal isomers.

*VII. B. 7. Trigonal **4***. The structure of the trigonal **4** isomer is shown in Figures 6, 7, and S1. Quantitative results are collected in Tables S15 and S22. The cluster's total interaction

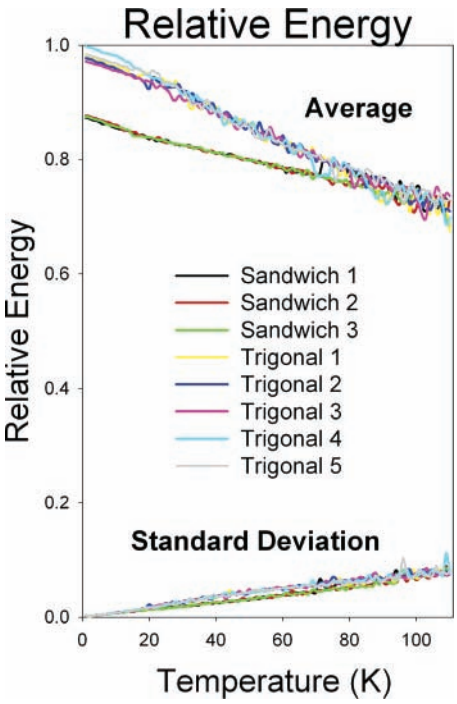

Figure 8. Temperature dependence of the total interaction energy and its standard deviation for the eight isomers. Energies are relative to the optimized energy of the trigonal 4 isomer; traces in the graph represent the average over all four potential energy surfaces. The legend relates isomers to their respective traces.

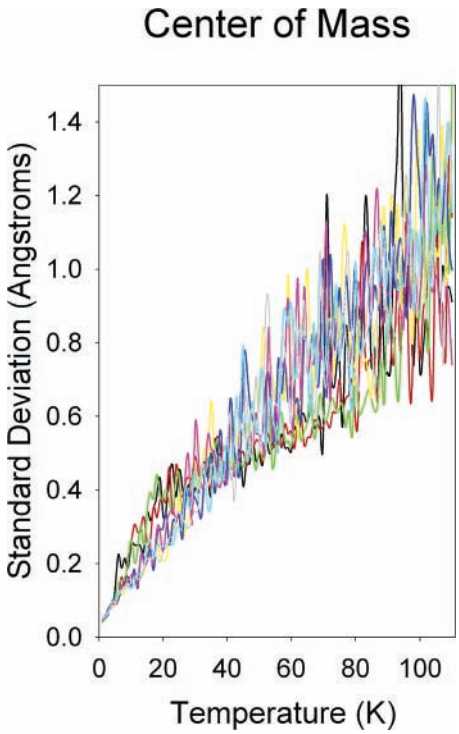

Figure 9. Temperature dependence of the standard deviation of the cyclohexane center-of-mass coordinates. The color scheme used to distinguish isomers is identical to that of Figure 8.

energy is distributed among C_6H_6, $C_6H_{12}-1$, and $C_6H_{12}-2$ in the approximate percentages 31%, 38%, and 31%. The axial cyclohexane molecule is located 4.770 Å from the coordinate system origin, with CM coordinates of (1.478, 0.202, 4.530) Å and a tilt of 43.8°. Its equatorial counterpart is centered at 5.826 Å from the origin, with CM coordinates of (4.569, 3.001, 2.014) Å and a molecular tilt of 69.0°. Both centers of mass lie above benzene's molecular plane. Quantitative results in Table S22 show that the structure is unique under average conditions at 2 K. Of the eight isomers, the trigonal **4** isomer is consistently *lowest* in energy (i.e., it represents the global energy minimum).

VII. B. 8. Trigonal 5. The structure of the trigonal **5** isomer is shown in Figures 6, 7, and S1. Quantitative results are collected in Tables S16 and S23. The cluster's total interaction energy is distributed among C_6H_6, $C_6H_{12}-1$, and $C_6H_{12}-2$ in the approximate percentages 33%, 38%, and 29%. The axial cyclohexane molecule is located 4.336 Å from the coordinate system origin, with CM coordinates of (1.173, 0.257, 4.167) Å and a tilt of 6.6°. Its equatorial counterpart is centered at 5.885 Å from the origin, with CM coordinates of (4.735, 3.121, 1.527) Å and a molecular tilt of 63.1°. Both centers of mass lie above benzene's molecular plane. Quantitative results in Table S23 confirm that the structure is unique at 2 K.

VII. C. Caloric Studies of the Trimer. In section V. D, temperature-dependent studies were described for the dimer cluster. In those studies, it was found that comparable information can be extracted by either averaging results from all four PES simulations at low resolution (in 1 K steps) or running the calculations at higher-temperature resolution on a single PES. For the trimer studies, we have adopted the former approach, averaging results of all four PESs, each at a temperature resolution of 1 K. Optimized mean structures were used as initial configurations for each of the eight isomers.

The temperature dependence of each isomer's total interaction energy is shown in Figure 8. Values in the figure are computed by first calculating the ratio of the temperature-dependent energy average to the global minimum for each PES; the results are then averaged. The temperature resolution of the simulations is 1 K. It is noteworthy that the average energy of the trigonal **4** isomer remains distinct at temperatures below ∼15 K, where it begins to merge with the other trigonal isomer energies. Furthermore, a definite separation between sandwich and trigonal isomer energies is maintained at temperatures below ∼70 K.

Standard deviations of the cyclohexane molecular centers of mass and of the atomic coordinates are plotted separately in Figures 9 and 10. Not surprisingly, the trend is an increase in center-of-mass standard deviation with temperature. More interesting are trends in the degree of fluctuation. Fluctuations in the center-of-mass standard deviations are negligible at temperatures below ∼6 K; thereafter, they increase with temperature, becoming significant at temperatures above ∼45 K.

At very low temperature, atomic position standard deviations are indistinguishable for the eight isomers (Figure 10). At ∼5 K, a noticeable separation is observed wherein traces of the sandwich isomers rise steeply, whereas those of the trigonal isomers rise at a slower rate. The two subsets of traces remain well-separated until the temperature reaches ∼45 K, where they begin to lose their distinct identities and finally merge at ∼60 K.

VIII. Application to the Benzene−Cyclohexane Trimer, $(C_6H_6)(C_6H_{12})_2$: Discussion

VIII. A. Isomers, Structures, and Energies. The data provide consistent witness to the coexistence of eight stable trimer isomers at low temperature (2 K). The distinctness of each isomer is confirmed by comparison of the optimized structures (Figures 6, 7, and S1) and is further supported by differences between total interaction and molecular stabilization energies.

To provide additional quantification, mean-squared atomic displacements were calculated for each of the isomer pairs. Results of this analysis are collected in Table 9. This analysis

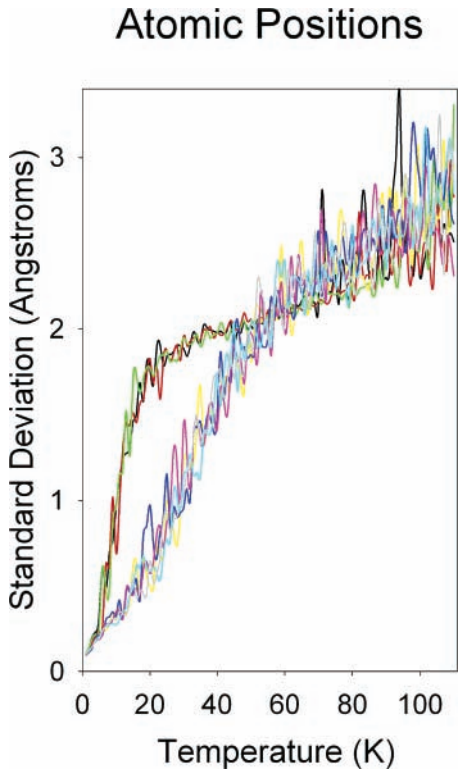

Figure 10. Temperature dependence of the standard deviation of the 36 cyclohexane atomic coordinates. The color scheme used to distinguish the isomers is identical to that of Figure 8.

takes into account that there exist $2!(24)(12)^2 = 6912$ equivalent sets of molecular coordinates for each trimer isomer. Tabulated are the minimum values of $\langle(\Delta r)^2\rangle$ for each pair, evaluated over all molecular permutation and symmetry combinations.

Values of $\langle(\Delta r)^2\rangle$ for sandwich−sandwich pairs are relatively small, reflecting similarity between the three sandwich isomers. This is not surprising, given that all three have nearly identical coordinates for $C_6H_{12}-1$; differences stem from the symmetry-related placement of $C_6H_{12}-2$. Also unsurprising is the large mean-square displacements for sandwich−trigonal pairs (>26 Å^2). Of the trigonal structures, trigonal **1**, **4**, and **5** are most similar: their molecular centers of mass reside in the same vicinity, but their cyclohexane moieties are oriented differently. Trigonal **2** and trigonal **3** show greater differences from the other isomers (>4.6 Å^2).

A comparison and ranking of the isomer interaction energies is provided in Table 10. Energies for each PES (columns 2−5) are relative to the optimized trigonal **4** energy for that PES; averages and standard deviations are shown in columns 6−7. Average rankings and standard deviations (with 1 representing minimum energy) are shown in columns 8−9. The last column contains overall rankings based on average relative energies. The data consistently identify trigonal **4** as the lowest energy isomer and the three sandwich structures as highest in energy in the order, *E*(sandwich **2**) < *E*(sandwich **3**) < *E*(sandwich **1**). Ordering of the remaining four trigonal isomers is not unambiguous, although the order in the last column of Table 10 is reasonable, based on trends in the data.

VIII. B. Relationship to Experimental Results. The trimer's resonance-enhanced two-photon one-color ultraviolet spectrum has been previously reported, measured through benzene's $B_{2u} \leftarrow A_{1g}$ 6^1_0 transition near 260 nm.[25] Although the raw spectrum contained fragmentation artifacts originating from the tetramer cluster, the application of spectral subtraction successfully removed evidence of fragmentation. The resulting (corrected) trimer spectrum is shown in Figure 11. The approach used to interpret the van der Waals progressions was discussed in section VI. C. Spectroscopic constants are identified here (in cm^{-1}) as a triplet ($\bar{\nu}_0$, $\bar{\nu}_e$, $\bar{\nu}_e\chi_e$).

The $(C_6H_6)(C_6H_{12})_2$ spectrum is characterized by a series of sharp features. An alternating pattern of the more intense features is obvious, probably indicating the presence of two distinct progressions. Five low-intensity features continue the progressions at higher energy. Analyzed as separate progressions, the spectroscopic constants are A = (−65.7, 16.4, 0.74) and B = (−57.8, 15.6, 0.8). Subscripts A and B in the Figure 11 peak labels distinguish the two progressions, while the numbers (0−4) identify the relevant vdW quantum number in the upper electronic state. All wavenumbers calculated from the spectroscopic constants fall within 0.1 cm^{-1} of observed values for the first mode. For the second mode, one predicted position differs from its experimental value by 1.26 cm^{-1}, which exceeds the spectral resolution (0.75 cm^{-1}).[25]

One possibility discussed in ref 25 is that the smaller-intensity subset (A) constitutes a hot band, originating 5.8 cm^{-1} above the ground-state zero point with excited-state spectroscopic constants of (−58.8, 16.0, 0.8). On the basis of intensity ratios between the two sequences (0.69), a vibrational temperature of 23 K in the ground state would be inferred. The second major possibility is that the two progressions originate from distinct subsets of isomers. The results of this study support the second interpretation.

The reproducibility and sharpness of spectroscopic features, combined with temperature-dependence results for both the dimer and trimer clusters, indicate that the *translational* temperature of experimental clusters is below 10 K. This is well below the *vibrational* temperature (23 K) required for the hot-band interpretation. By itself, this is not fatal to the hot-band interpretation, however, because translational and vibrational temperatures need not be identical for clusters in a supersonic jet.

The coexistence of two disparate classes (sandwich and trigonal) of trimer isomers provides significant support to the hypothesis that two independent van der Waals series originate from distinct classes of isomers. In general, it is expected that a C_6H_6 molecule with greater stabilization energy will be associated with a spectral feature shifted further to the red. (In these spectra, the site energy of C_6H_6 (not cyclohexane) is of particular relevance, because the vibronic transitions are localized on the benzene moiety.) Our MC results indicate the coexistence of three sandwich and five trigonal isomers; the ratio is 0.6. Benzene's stabilization energy in the sandwich isomers is greater than in the trigonal isomers. On the Jorgensen PES, for example, the benzene molecule experiences an average stabilization of -12.375 ± 0.002 kJ mol^{-1} in the sandwich isomers, but only -9.41 ± 0.44 kJ mol^{-1} in the trigonal structures.

These observations are consistent with assignment of the A series (greater red shift, lower intensity) to the sandwich group and the B series to the trigonal group. If these assignments are correct, it is likely that each isomer has only one vdW mode represented in the R2PI spectrum. Furthermore, isomers within each class probably have comparable transition energies, with differences not exceeding the experimental resolution, 0.75 cm^{-1}. Presumably, this conclusion could be tested via electronic structure calculations. Unfortunately, software-imposed limitations in hard disk usage proved fatal to trimer MP2 frequency calculations.[28]

VIII. C. Structural Transitions and the Potential Energy Surface. Caloric simulations identify two temperature ranges

TABLE 9: Mean-Squared Atomic Displacements between Isomer Pairs[a]

$\langle(\Delta r)^2\rangle$/Å^2 standard → guess ↓	sand **1**	sand **2**	sand **3**	trig **1**	trig **2**	trig **3**	trig **4**
sand **2**	2.5529	0.0000					
sand **3**	2.0994	2.1271	0.0000				
trig **1**	27.3455	26.6492	26.6974	0.0000			
trig **2**	>30	>30	>30	4.8600	0.0000		
trig **3**	>30	>30	>30	10.0626	4.6480	0.0000	
trig **4**	>30	>30	>30	1.8228	4.9714	7.2911	0.0000
trig **5**	>30	>30	>30	2.8245	4.8390	7.1638	1.7561

[a] Smaller values of $\langle\Delta r^2\rangle$ reflect greater similarity between isomeric structures.

TABLE 10: Relative Energies and Rankings of the Eight Trimer Isomers

	Jorgensen rel *E*	Shi (3) rel *E*	van de Waal rel *E*	Williams rel *E*	average rel *E*	stdev rel *E*	average rank	std rank	energy rank
trigonal **4**	1.0000	1.0000	1.0000	1.0000	1.000	0.000	1.0	0.0	1
trigonal **5**	0.9943	0.9763	0.9892	0.9863	0.987	0.008	2.8	1.0	2
trigonal **1**	0.9798	0.9846	0.9829	0.9852	0.983	0.002	3.3	1.3	3
trigonal **2**	0.9619	0.9774	0.9928	0.9850	0.979	0.013	3.3	1.0	4
trigonal **3**	0.9595	0.9708	0.9861	0.9798	0.974	0.012	4.8	0.5	5
sandwich **2**	0.8374	0.8608	0.9120	0.8998	0.878	0.034	6.0	0.0	6
sandwich **3**	0.8360	0.8595	0.9109	0.8988	0.876	0.035	7.0	0.0	7
sandwich **1**	0.8334	0.8570	0.9089	0.8970	0.874	0.035	8.0	0.0	8

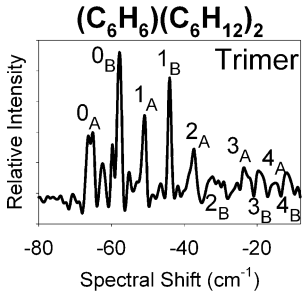

Figure 11. Resonance-enhanced two-photon ionization spectrum of the trimer, measured through benzene's $B_{2u} \leftarrow A_{1g}$ 6^1_0 vibronic transition (ref 25). The spectrum shown was cleaned by spectral subtraction to eliminate artifacts of fragmentation from larger clusters. Peaks are labeled to identify two independent progressions (A, B); the numbers (0−4) identify the vdW quantum number in the upper electronic state.

in which transitions between isomeric forms may occur. The potential energy of trigonal **4** is less than and distinct from all other isomers at temperatures below ∼15 K (Figure 8). In the same figure, it is observed that the sandwich and trigonal energies are separated below $T \approx 60$ K. Standard deviations of cyclohexane's atomic positions are also disparate between the sandwich and trigonal isomer forms from 5 K up to temperatures in the range 45−60 K (Figure 10).

These patterns indicate that all structures are rigid and unique below 5 K. In the 5−15 K range, an increase is observed in thermal activity: molecular centers of mass experience small increases in their standard deviations, while the atomic coordinate standard deviations increase more dramatically. Above 15 K, both center-of-mass movement and rotational activity continue to increase with temperature. The isolation of trigonal **4**'s energy trace (Figure 8) from the other isomer energies attests to this isomer's uniqueness below 15 K. The trigonal-versus-sandwich differences with respect to atomic standard deviations (Figure 10) supports the coexistence of two isomer classes at temperatures below 60 K.

To explore this further, additional isothermal simulations were pursued on the Jorgensen PES at temperatures of 10, 20, 40, and 70 K, using a subset of 4 optimized isomers as starting configurations. For each isomer−temperature combination, Table 11 contains the mean-square displacement ($\langle\langle(\Delta r)^2\rangle$/Å^2) of the thermally averaged structure relative to the 8 (original) isomer structures. These simulations were carried out using 1000 isothermal steps, each consisting of 2×10^4 trial moves. Averaging was applied only over the last 500 isothermal cycles (10^7 MC trials). Four isomers were arbitrarily selected as representative of their classes: sandwich **2**−**3** and trigonal **3**−**4**. The boldfaced entries in Table 11 represent a "before and after" picture of the mean-square displacement, whereas the remaining entries indicate how closely the thermally averaged result approximates the ideal structure of a different isomer.

The results in Table 11 are best interpreted with reference to the data in Table 9 and relevant values for the individual isomers (Tables 8 and S17−S23). The following summary points are germane: (1) The range of $\langle(\Delta r)^2\rangle$/Å^2 values for the Jorgensen PES (comparing one isomer's Jorgensen-optimized structure to its *mean* optimized structure) is 0.0115−0.0362, with an average of 0.0193 ± 0.0099. (2) Typical values for different isomer combinations *within* the sandwich group (e.g., sandwich **1**−sandwich **2**) are 2.3 ± 0.3. (3) For distinct pairs within the trigonal group, the differences are more diverse, ranging from 1.8 to 10.1, with an average value of 5.0 ± 2.6. (4) For cross-group isomer pairs (e.g., trigonal **3**−sandwich **2**), the value of $\langle(\Delta r)^2\rangle$/Å^2 is greater than 25. These ranges offer a useful framework for interpreting the results.

The greatest significance of the data in Table 11 lies in the trends that are observed. At 2 K, the sandwich **2** isomer is close to its optimal configuration and is clearly distinct from the other sandwich isomers. At 10, 20, and 40 K, the structure still assumes a stacked form, but the mean structure no longer parrots the original. By 70 K, the structure has been converted from sandwich to trigonal. The same pattern is observed for the sandwich **3** isomer. The pattern points to a low conversion barrier between sandwich structures (<10 K) and a higher barrier between sandwich and trigonal isomeric forms (between 40 and 70 K).

The trigonal **3** structure (unique at 2 K) no longer remains distinct from the other trigonal isomers at 20 K, where it more closely resembles trigonal **5**'s original structure. At 40 and 70 K, the structure looks *generically* trigonal. The pattern for trigonal **4** is similar, except that the isomer clearly maintains its original configuration through temperatures of 10 K. At 20

TABLE 11: Mean-Squared Displacements of Thermally Averaged Structures[a]

$\langle(\Delta r)^2\rangle$/Å^2 standard → average ↓	sand **1**	sand **2**	sand **3**	trig **1**	trig **2**	trig **3**	trig **4**	trig **5**
sand **2** (2 K)	2.60	**0.01**	2.15	26.2	>30	>30	>30	>30
sand **2** (10 K)	1.97	**2.10**	1.82	>30	>30	>30	>30	>30
sand **2** (20 K)	2.10	**2.21**	1.68	>30	>30	>30	>30	>30
sand **2** (40 K)	2.07	**2.26**	2.22	>30	>30	>30	>30	>30
sand **2** (70 K)	>30	>**30**	>30	22.7	12.4	7.18	18.7	21.8
sand **3** (2 K)	2.15	2.12	**0.01**	26.1	>30	>30	>30	>30
sand **3** (10 K)	1.95	1.99	**1.57**	>30	>30	>30	>30	>30
sand **3** (20 K)	2.83	2.88	**1.62**	>30	>30	>30	>30	>30
sand **3** (40 K)	2.53	2.63	**1.88**	>30	>30	>30	>30	>30
sand **3** (70 K)	25.1	26.0	**25.2**	4.78	4.51	5.27	5.98	5.12
trig **3** (2 K)	>30	>30	>30	9.25	4.50	**0.03**	6.58	6.41
trig **3** (10 K)	>30	>30	>30	10.2	4.94	**1.51**	8.49	8.71
trig **3** (20 K)	>30	>30	>30	3.68	3.80	**5.50**	2.24	0.64
trig **3** (40 K)	>30	>30	>30	9.35	4.36	**3.29**	7.22	7.34
trig **3** (70 K)	>30	>30	>30	13.3	8.47	**6.73**	11.2	14.0
trig **4** (2 K)	>30	>30	>30	1.80	4.90	7.30	**0.01**	1.78
trig **4** (10 K)	>30	>30	>30	1.81	4.96	7.30	**0.01**	1.76
trig **4** (20 K)	>30	>30	>30	2.69	5.39	7.58	**1.95**	0.06
trig **4** (40 K)	>30	>30	>30	5.57	3.04	6.51	**5.28**	4.61
trig **4** (70 K)	>30	>30	>30	11.94	5.90	6.01	**12.4**	12.6

[a] The results for four isomers (sandwiches **2**−**3** and trigonal **3**−**4**) are shown at five different simulation temperatures (2, 10, 20, 40, and 70 K), relative to standard structures. All values are computed on the Jorgensen PES. Entries corresponding to the original isomer of each simulation are in boldface.

K, the average structure mimics that of trigonal **5**'s optimized structure. The significance of this is unclear, though it is remarkable that both trigonal **3** and **4** display this behavior at 20 K. From the data, it is inferred that the barrier to conversion between trigonal isomers is less than 20 K, at least in some cases. It is interesting to note that none of the trigonal structures are observed to assume a sandwich structure upon heating (an expected result, given the greater structural entropy of the trigonal isomers).

IX. Conclusions

Well-chosen Monte Carlo computational strategies can be implemented to gain information about solvation cluster systems, exemplified by $(C_6H_6)(C_6H_{12})_n$. Beginning with a random configuration, clusters are heated to 100 K and then cooled in two steps to 0.01 K. Resulting structures are analyzed on the basis of symmetry operations to isolate and identify independent isomers. Follow-up simulated annealing studies determine each isomer's minimum energy and optimal configuration. Isothermal simulations at 2 K explore energetic and structural characteristics of the cluster population generated in cold supersonic expansions. Simulations that monitor temperature-dependent data are implemented to discern characteristics of the cluster's potential energy surface.

The strategy was first applied to the benzene−cyclohexane dimer. Four different PES parameter sets were used in independent Monte Carlo simulations. All support the same conclusions. The dimer has a single isomeric form with a parallel-displaced structure. Isothermal averaging simulations at 2 K find that low-temperature dimer clusters are rigid, with average structures mimicking the optimized structure. Caloric studies indicate two transitional temperatures near 10 and 100 K. Below 10 K, dimer structures are rigid. Between the two limits, the relative centers of mass are minimally mobile, but rotational activity is increased. Beyond 100 K, both translational and rotational motions are active in a fluxional cluster.

Electronic structure calculations (MP2/6-31g(d)) provide independent confirmation of the dimer's configuration. Frequency calculations that include zero-point corrections to the electronic energy predict a dimerization energy of -8 kJ mol^{-1} at low temperature and identify the van der Waals mode observed in R2PI spectra: it is the lowest-energy vdW mode, characterized by simultaneous molecular twisting (in opposite directions) of the C_6H_6 and C_6H_{12} molecules.

The benzene−cyclohexane trimer, $(C_6H_6)(C_6H_{12})_2$, was also investigated. Eight stable low-temperature isomers are identified, subdivided into *sandwich* and *trigonal* groups. The three sandwich isomers have stacked arrangements, with two equivalent cyclohexane molecules (related by S_6, S_3, or σ_h symmetry) parallel to the benzene sandwich center. These are higher in energy than the five trigonal isomers. In the trigonal structures, the cyclohexane moieties are inequivalent, with the axial member experiencing the greater interaction/stabilization energy. Two classes of trimer isomers are consistent with the two distinct van der Waals progressions observed in the trimer's R2PI spectrum. Caloric studies reveal that the isomeric structures are rigid at temperatures below 5 K; as the temperature approaches 15 K, molecular rotational motion begins to increase. By 60 K, distinctions between trigonal and sandwich classes become blurred as temperature dependence studies reflect increasingly fluxional clusters.

In our judgment, the search for unique trimer isomers in this study was extensive. Nevertheless, the possibility exists that one or more stable isomers may be identified by future study. Even given this possibility, it is unlikely that identification of additional isomers will substantively affect the description of the trimer's PES resulting from this work.

With appropriate adaptation, the general approach adopted for this study can be applied to a broad range of solvent−solute cluster systems. Specific modifications might involve the adaptation of PES parameters to include atoms other than carbon and hydrogen and the implementation of additional symmetry operations. A final comment is in order: The method used for symmetry analysis was brute-force in nature. Each structural comparison involved calculation of $n!(24)(12)^n$ mean-squared atomic coordinate displacements, where n is the number of cyclohexane molecules in the cluster. Computationally, this is feasible for small clusters. However, for $n > 5$, a more elegant approach will be needed to address computational time constraints.

The general application of our computational strategy to mixed solvent−solute molecular clusters should yield accurate and useful results. In our laboratory, continuing work focuses on application of the methodology to $(C_6H_6)(C_6H_{12})_n$, $n \geq 3$.

Acknowledgment. D.C.E. received partial funding for this work from the Robert A. Welch Foundation (grant AI-1392). J.A.R. and D.A.T. were partially supported by Welch Foundation undergraduate stipends. Ben Stotts provided technical assistance with the installation and configuration of computer operating systems and software.

Supporting Information Available: Tables S1−S2, S4−S5, and S7 contain complete potential energy parameters for the four PESs; Tables S3, S6, and S8 contain the corresponding bond distances and the atomic coordinates of symmetry-unique atoms for C_6H_6 and C_6H_{12} in their standard orientations. The optimized molecular coordinates identified by each PES (see Table 7) are collected for seven trimer isomers in Tables S9−S16. Key results (see Table 8) are tabulated for seven isomers in Tables S17−S23. Table S24 contains D_{6h} symmetry transformations in Cartesian coordinates, and Table S25 presents transformation matrices for Euler rotations of coordinates. Figure S1 presents all eight trimer isomers from the perspective of the $+x$ axis, complementing Figures 6−7. This material is available free of charge via the Internet at http://pubs.acs.org.

References and Notes

(1) Börnsen, K. O.; Lin, S. H.; Selzle, H. L.; Schlag, E. W. *J. Chem. Phys.* **1989**, *90*, 1299.
(2) Menapace, J. A.; Bernstein, E. R. *J. Phys. Chem.* **1987**, *91*, 2843.
(3) Easter, D. C.; Harris, J. P.; Langendorf, M.; Mellott, J.; Neel, M.; Weiss, T. *J. Phys. Chem. A* **1998**, *102*, 10032.
(4) Easter, D. C.; Baronavski, A. P.; Hawley, M. *J. Chem. Phys.* **1993**, *99*, 4942.
(5) Easter, D. C.; Khoury, J. T.; Whetten, R. L. *J. Chem. Phys.* **1992**, *97*, 1675.
(6) Easter, D. C.; Li, X.; Whetten, R. L. *J. Chem. Phys.* **1991**, *95*, 6362.
(7) Easter, D. C.; Whetten, R. L.; Wessel, J. E. *J. Chem. Phys.* **1991**, *94*, 3347.
(8) Börnsen, K. O.; Selzle, H. L.; Schlag, E. W. *J. Chem. Phys*. **1986**, *85*, 1726.
(9) Schlag, E. W.; Selzle, H. L. *J. Chem. Soc., Faraday Trans.* **1990**, *86*, 2511.
(10) Iimori, T.; Ohshima, Y. *J. Chem. Phys.* **2001**, *114*, 2867.
(11) Iimori, T.; Ohshima, Y. *J. Chem. Phys.* **2002**, *117*, 3656.
(12) Iimori, T.; Aoki, Y.; Ohshima, Y. *J. Chem. Phys.* **2002**, *117*, 3675.
(13) Easter, D. C. *J. Phys. Chem. A* **2003**, *107*, 2148.
(14) Easter, D. C. *J. Phys. Chem. A* **2003**, *107*, 7733.
(15) Williams, D. E. *Acta Crystallogr., Sect. A* **1980**, *36*, 715.
(16) van de Waal, B. W. *J. Phys. Chem*. **1983**, *79*, 3948.
(17) van de Waal, B. W. *Chem. Phys. Lett.* **1986**, *123*, 69.
(18) Dulles, F. J.; Bartell, L. S. *J. Phys. Chem*. **1995**, *99*, 17100.
(19) Easter, D. C. *J. Cluster Sci.* **2004**, *15*, 33.
(20) Williams, D. E.; Starr, T. L. *Comput. Chem*. **1977**, *1*, 173.
(21) Jorgensen, W. L.; Severance, D. L. *J. Am. Chem. Soc*. **1990**, *112*, 4768.
(22) Karlström, G.; Linse, P.; Wallqvist, A.; Jönsson, B. *J. Am. Chem. Soc*. **1983**, *105*, 3777.
(23) Shi, X.; Bartell, L. S. *J. Phys. Chem*. **1988**, *92*, 5667.
(24) El-Shall, M. S.; Whetten, R. L. *Chem. Phys. Lett*. **1989**, *163*, 41.
(25) Easter, D. C.; Davis, K. A. *Phys. Chem. Lett.* **2003**, *380*, 471.
(26) Arfken, G. B.; Weber, H. J. *Mathematical Methods for Physicists*, 4th ed.; Academic Press: New York, 1995; p 188.
(27) Frenkel, D.; Smit, B. *Understanding Molecular Simulation: From Algorithms to Applications*; Academic Press: New York, 1996; p 23.
(28) Frisch, M. J.; Trucks, G. W.; Schlegel, H. B.; Scuseria, G. E.; Robb, M. A.; Cheeseman, J. R.; Montgomery, J. A., Jr.; Vreven, T.; Kudin, K. N.; Burant, J. C.; Millam, J. M.; Iyengar, S. S.; Tomasi, J.; Barone, V.; Mennucci, B.; Cossi, M.; Scalmani, G.; Rega, N.; Petersson, G. A.; Nakatsuji, H.; Hada, M.; Ehara, M.; Toyota, K.; Fukuda, R.; Hasegawa, J.; Ishida, M.; Nakajima, T.; Honda, Y.; Kitao, O.; Nakai, H.; Klene, M.; Li, X.; Knox, J. E.; Hratchian, H. P.; Cross, J. B.; Adamo, C.; Jaramillo, J.; Gomperts, R.; Stratmann, R. E.; Yazyev, O.; Austin, A. J.; Cammi, R.; Pomelli, C.; Ochterski, J. W.; Ayala, P. Y.; Morokuma, K.; Voth, G. A.; Salvador, P.; Dannenberg, J. J.; Zakrzewski, V. G.; Dapprich, S.; Daniels, A. D.; Strain, M. C.; Farkas, O.; Malick, D. K.; Rabuck, A. D.; Raghavachari, K.; Foresman, J. B.; Ortiz, J. V.; Cui, Q.; Baboul, A. G.; Clifford, S.; Cioslowski, J.; Stefanov, B. B.; Liu, G.; Liashenko, A.; Piskorz, P.; Komaromi, I.; Martin, R. L.; Fox, D. J.; Keith, T.; Al-Laham, M. A.; Peng, C. Y.; Nanayakkara, A.; Challacombe, M.; Gill, P. M. W.; Johnson, B.; Chen, W.; Wong, M. W.; Gonzalez, C.; Pople, J. A. *Gaussian 03*, revision B.02; Gaussian, Inc.: Pittsburgh, PA, 2003.
(29) Foresman, J. B.; Frisch, Æ. *Exploring Chemistry with Electronic Structure Calculations*, 2nd ed.; Gaussian: Pittsburgh, 1996; p 64.